(18) AFOSR-TR-79-0692

(19)

LEVEL II

(8)

(9)

Semi-Annual Technical Report, No. 1

1 October 1978 - 31 March 1979

ARPA Order:	3291-21
Program Code:	9D60
Contractor:	Saint Louis University 405 292
Effective Date of Contract:	1 October 1978 (11) 23 Apr 79
Contract Expiration Date:	30 September 1980
Amount of Contract:	$165,000 (12) 85p.
Contract Number:	F49620-79-C-0025
Principal Investigators:	(10) Otto W. Nuttli Brian J. Mitchell
Phone:	314-658-3124 or 3123
Program Manager:	Brian J. Mitchell
Phone:	314-658-3123
Short Title:	(6) Research in Seismology.

Sponsered by

Advanced Research Projects Agency (DOD)

ARPA Order No. 3291-21

Monitored by AFOSR Under Contract F49620-79-C-0025 (15)

405 292

LB

A

Table of Contents:

Q sub beta

B

Technical Report Summary

The data from short-period WWSSN seismograms were used to study the excitation and attenuation of 1-Hz crustal phases (P, Pg, Sn and Lg) in southern Asia. The data show that the attenuation in southern Asis varies laterally, but that in general it is less than in Iran and the western United States, and greater than in eastern North America and central Asia. The most severe attenuation occurs in northern India, northern Pakistan and Afghanistan, where it is comparable to the values found for Iran and the western United States.

The only crustal phase with a sharp onset for southern Asia earthquakes is P (or Pn). Thus it will have to be used for locating earthquakes and explosions. For an m_b = 4.0 event this P phase (vertical component) has a ground amplitude of at least 1 millimicron to distances of 3500 km. For purely detection purposes, Pg and Lg will have larger amplitudes to distances of up to 1000 km, but their amplitudes become less than those of P and Sn at distances beyond 1000 km in southern Asia.

The amplitude variations of P with epicentral distance in southern Asia departs from the standard Gutenberg-Richter relation by as much as 0.5 m_b units at distances of 500 to 2500 km. Thus the Gutenberg-Richter calibration function should not be used at these distances to determine m_b, or to estimate yield of explosions.

From recently published Soviet studies it appears that the attenuation of seismic crustal phases in central Asia is more similar to that in

eastern North America than to that in southern Asia. Thus Lg should be useful for detecting low-magnitude events out to distances of 2000 km in the interior of the USSR. However, Lg cannot be used for accurate source location, for which one will have to continue to use arrival times of P.

Methods for inverting higher-mode attenuation data in the period range 4-10 seconds are being developed and have been applied successfully to Rayleigh wave data in the central United States. The combination of fundamental- and higher-mode amplitude spectra make it possible to simultaneously solve for source depth and crustal Q models.

Higher-mode data, both in the period range 5-10 seconds and at 1 second (Lg) have been combined with fundamental-mode data to yield new frequency-dependent Q models for eastern North America. A variation of shear wave Q with frequency (ω) and depth (z) is assumed such that $Q_\beta(z,\omega) = C(z)\omega^\alpha$ where α is constant. The results indicate that the case $\alpha = 0$ (a frequency-independent Q model) do not explain the data very well. The best fit to the entire data set for a single α value for all periods occurs when $\alpha = 0.3$. Better fits are achieved when α is constant (between 0.0 and 0.2) over the period range 5-40 seconds and attain greater values for shorter periods.

Initial studies of higher modes in Iran and Turkey suggest that crustal Q values are very low and that intrinsic anelasticity is more important than scattering of seismic surface waves in the period range 4-10 seconds.

EXCITATION AND ATTENUATION OF SHORT-PERIOD CRUSTAL PHASES IN SOUTHERN ASIA

by

Otto W. Nuttli

INTRODUCTION

Earthquakes in Szechwan Province and Tibet, which occur in the border region separating central from southern Asia, were used to study the excitation and attenuation of short-period crustal phases in southern Asia. The region is one of complex geology and rugged topography, where strong attenuation of short-period crustal phases and large variations in wave amplitude might be expected. One of the purposes of this study is to specify the amplitudes of the waves P (or Pn), Pg, Sn and Lg for an earthquake of a given magnitude as a function of epicentral distance, and thus to determine which of the crustal phases is best suited for detection of small-to-intermediate magnitude seismic events in a particular distance range.

Most of the data for the study came from the WWSSN seismograms of the stations KBL (Kaboul, Afghanistan), QUE (Quetta, Pakistan) and CHG (Chengmai, Thailand), for which we possess a fairly complete set of records for the years 1971-1972. Also used were data from SHI (Shiraz, Iran), NIL (Nilore, Pakistan), KOD (Kodaikanal, India) and SHL (Shillong, India), for which we have seismograms for selected events. Additional seismograms have been on order since November 1978, but they have not been delivered as of April 1979. Figure 1

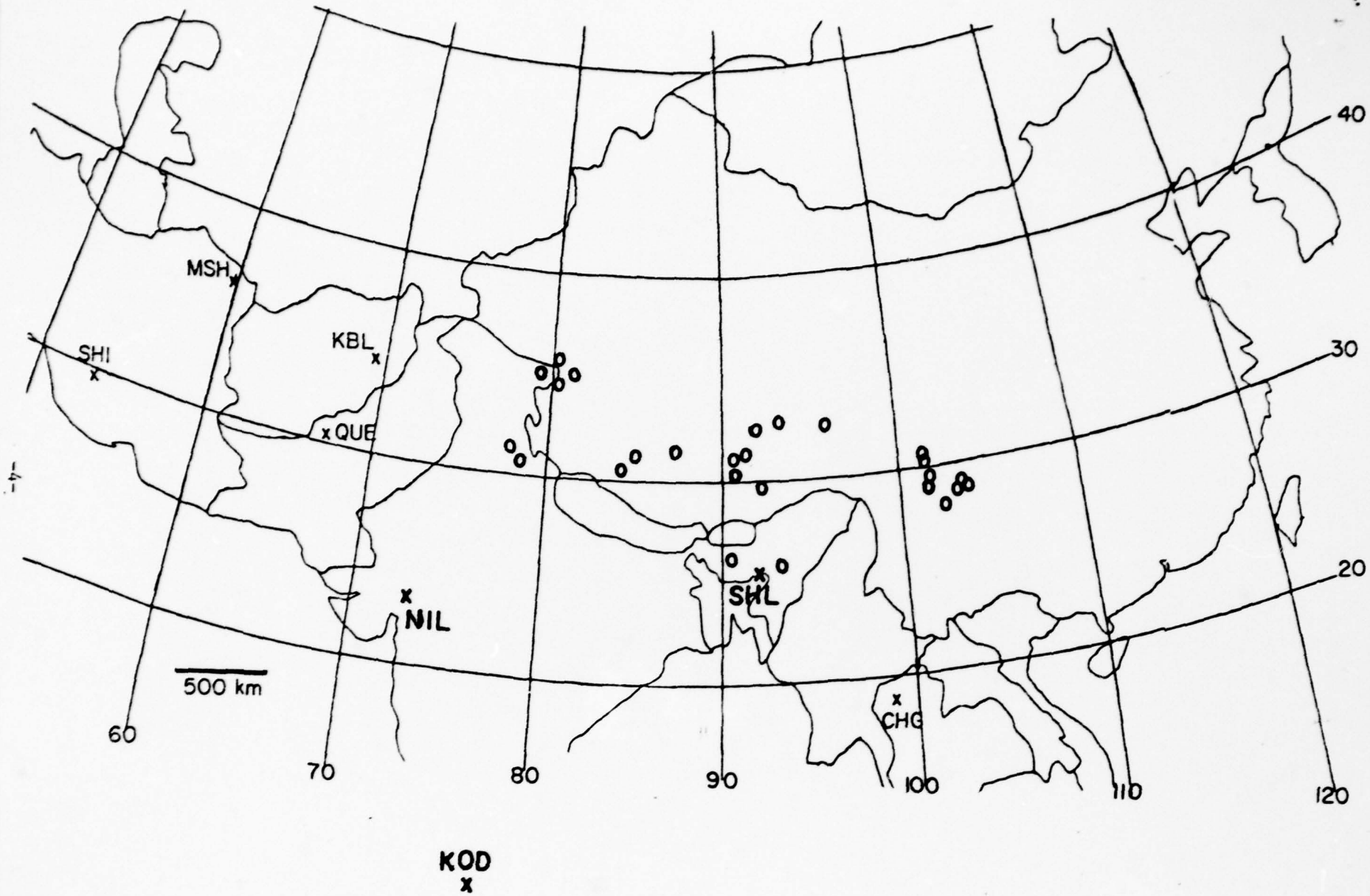

Figure 1. Location of earthquakes (circles) and seismograph stations (crosses) used in this study.

shows the location of the earthquake epicenters and of the stations used in the analysis.

METHODS OF DATA REDUCTION

All the earthquakes utilized in the study were reported in the Bulletin of the International Seismological Centre. The ISC assigned body-wave magnitude (m_b) values to the earthquakes on the basis of teleseismic P-wave amplitudes, which are completely independent of the data considered in this study.

The amplitudes of P (or Pn), Pg, Sn and Lg were measured on the vertical-component seismograms, and of Pg, Sn and Lg on the horizontal-component seismograms as well. After correction for instrument magnification the amplitudes were equalized to those of an m_b = 5.0 earthquake on the assumption that the logarithm of the amplitude of these waves at 1-sec period scales directly as m_b.

Horizontal-component amplitude data were combined with vertical-component data on the basis of previous observations that the resultant horizontal Pg amplitude is approximately equal to that of the vertical component, and that the resultant horizontal Lg amplitude is approximately twice that of the vertical-component. Inasmuch as the relation between the resultant horizontal and the vertical-component Sn amplitude is unknown, the two components of the Sn motion were considered separately.

In previous studies Nuttli (1973, 1978) presented far-field Lg amplitude data which could be extrapolated back by theory to 1 km epicentral distance. Assuming a point-source model of Lg radiation, the Lg data for m_b = 5.0 earthquakes in both northeastern America and Iran extrapolate back to a value of 800 microns at 1 km distance.

This number should not be taken as a measure of the Lg vertical-component ground motion at 1 km distance for 1-sec period waves, but rather as a source-related value which can be used to estimate Lg ground motion at distances of 50 km and greater. This can be done by using a theoretical equation for the attenuation of Lg surface waves, taking account of geometrical spreading, dispersion and anelastic attenuation or absorption.

From the observation that the extrapolation of the Lg data to 1 km is independent of source region, it becomes possible to estimate the average value of the absorption coefficient between the epicenter and station from a single amplitude value. Using a family of curves with absorption coefficient as parameter, the average value of the absorption coefficient for a path from the epicenter to the station can be estimated by plotting the equalized amplitude (to $m_b = 5.0$) versus epicentral distance and observing the curve, corresponding to a particular value of the absorption coefficient, on which the data point falls.

The amplitude variation of Pn and P waves at distances of about 500 to 3500 km does not follow a simple law, but rather depends on the velocity variation with depth in the upper mantle to depths of about 1000 km. Because no simple theoretical or empirical equation can be found to describe the amplitude behavior at these distances, the amplitude data were averaged over a 250 km distance interval and a smooth curve was drawn through the average values to describe the variation of amplitude with distance.

The amplitudes of Pg and Sn are observed to decrease monotonically with epicentral distance. Rather than attempt to fit these data with theoretical curves, it is customary to fit them with empirical straight-line curves on a plot of the logarithm of the amplitude versus the logarithm of the epicentral distance. The slopes of the curves are measures of the attenuation of Pg and Sn, and the intercepts a measure of the source excitation for an m_b = 5.0 event.

For some paths in southern Asia, 1-sec period Lg waves could not be observed on the seismograms, but waves of period 1.5 to 3 sec could be seen. In such cases the amplitudes of the longer period waves were reduced to those of 1-sec period waves by assuming that the Lg spectrum had a slope of 2 for periods of 1 to 3 sec. Thus the amplitude of a 1.5 sec period wave was divided by 2.3, of a 2-sec period wave by 4.0 and of a 3-sec period wave by 9.2 to reduce the amplitudes to those of 1-sec period waves. This procedure can be justified if the corner period for Lg waves from earthquakes of m_b = 5.0 is greater than or equal to 3 sec. For earthquakes for which both 1-sec and longer period Lg waves could be observed, the reduced amplitudes of the longer period waves were found to be approximately equal to the observed amplitudes of the 1-sec period waves, justifying the assumption.

AMPLITUDES OF Pn AND P WAVES

Figure 2 shows the logarithm of the vertical component of Pn and P waves plotted as a function of epicentral distance. Also shown on the curve are the logarthmic average of the amplitude for 250 km intervals (dashed horizontal lines) and a smooth curve drawn through the average values. The smooth curve can be taken to represent the average amplitude of Pn and P (vertical component) in southern Asia for an m_b = 5.0 earthquake. The scatter in the data is appreciable, amounting to as much as ±0.5 m_b units over most of the distance interval of 500 to 3500 km.

Figure 3 compares the average amplitude curve of Figure 2 for southern Asia with the Gutenberg-Richter (1956) amplitude curve, obtained from their body-wave magnitude calibration function, and with amplitude-distance data equalized to m_b = 5.0 obtained by Nuttli (1971) from a study of the amplitudes of P waves from nuclear explosions. At distances of 500 to 2300 km the Gutenberg-Richter curve differs appreciably from the curve obtained for southern Asia. At distances of 2300-3500 km the differences are smaller, but the Gutenberg-Richter curve on the average tends to have amplitudes about 0.2 to 0.3 m_b units larger. The nuclear explosion data, on the other hand, agree remarkably well with the southern Asia data at distances of 1950 to 3150 km, and differ by no more than 0.2 m_b units at distances of 3150 to 3500 km.

Figure 4 presents the P-wave amplitude deviations, in m_b units, for earthquakes in Tibet and the surrounding regions. The number in parenthesis is the number of earthquakes used to obtain

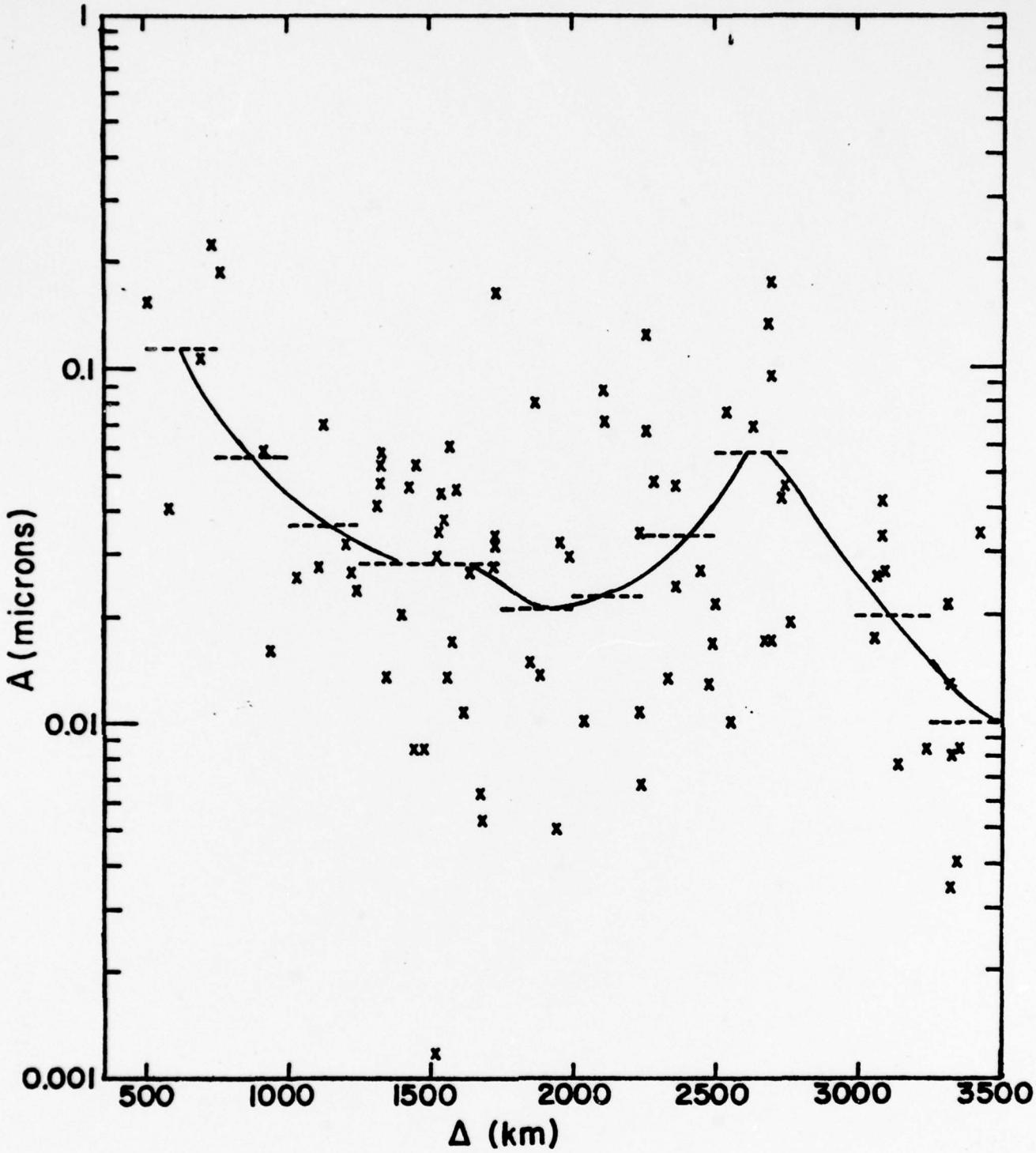

Figure 2. Amplitudes of vertical-component, 1-sec period P-wave motion equalized to an m_b = 5.0 earthquake. The dashed lines are logarithmic averages of the amplitude data over 250-km intervals. The solid-line curve is a smoothed curve drawn through the average values.

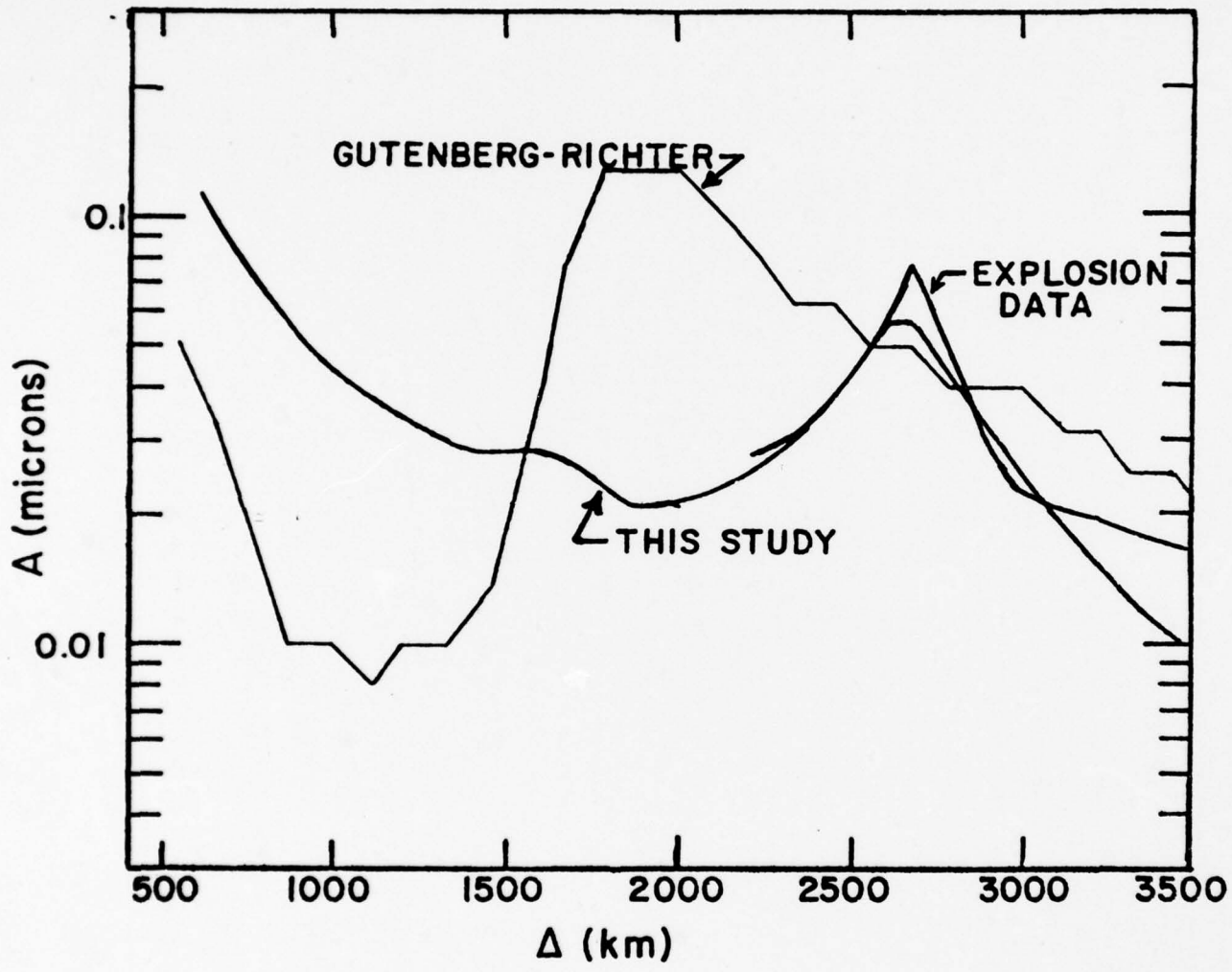

Figure 3. Amplitude curves for vertical-component, 1-sec period P-wave motion equalized to an m_b = 5.0 earthquake. Note the large departures between the Gutenberg-Richter (1956) curve and that obtained from the data for southern Asia. The nuclear explosion curve is from Nuttli (1971).

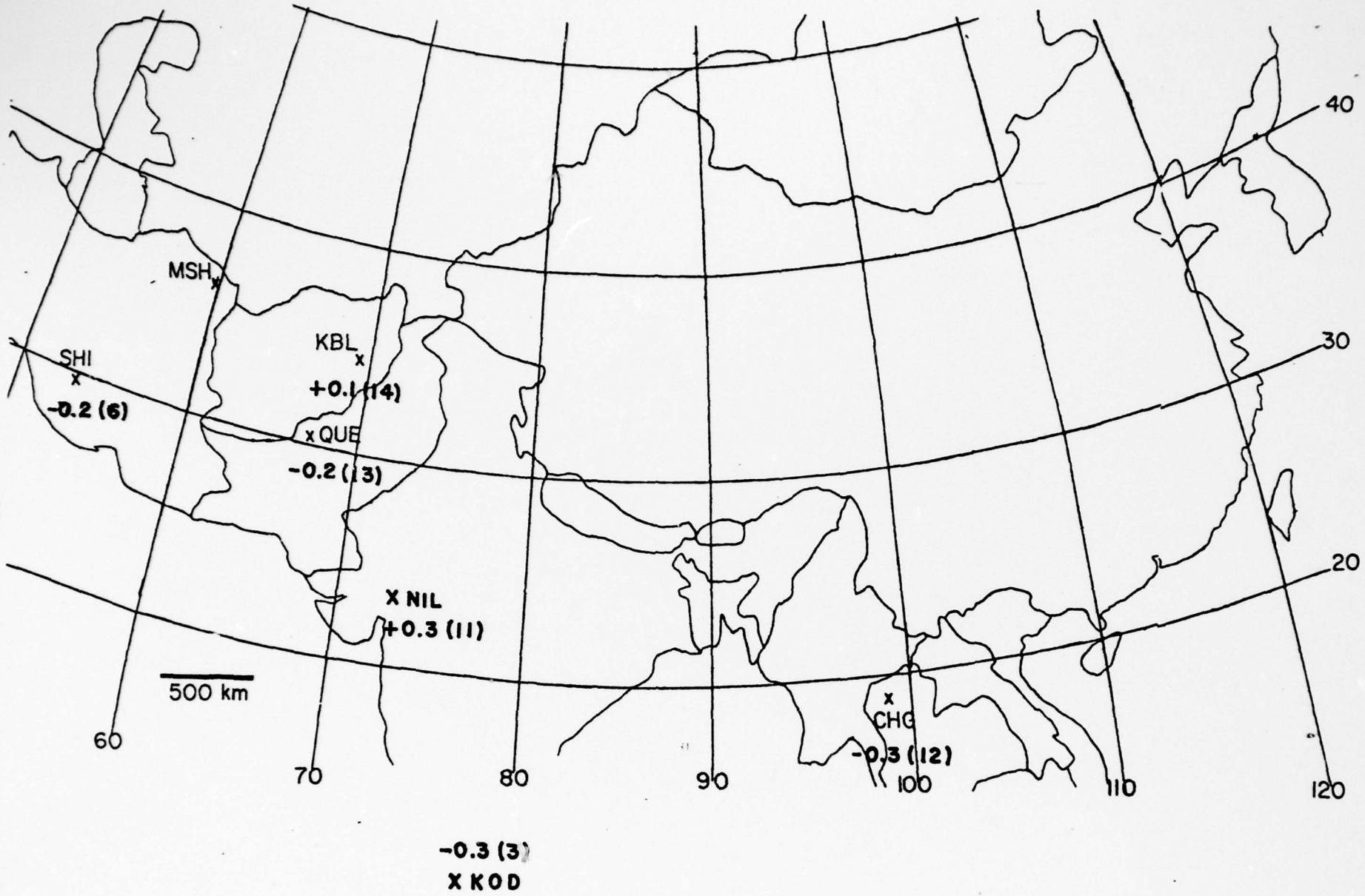

Figure 4. Average P-wave amplitude deviations, in m_b units, for earthquakes in Tibet. The number in parentheses refers to the number of observations.

the average amplitude deviation. A positive value of the amplitude deviation indicates that the observed amplitudes are greater than expected, and a negative value that the observed amplitudes are smaller than expected. The figure shows that NIL has amplitudes 2.0 times (0.3 m_b units) larger than expected, and KBL has amplitudes 1.3 times (0.1 m_n unit) larger than expected. On the other hand, observed amplitudes at SHI and QUE are 0.63 of the expected value, and KOD and CHG 0.50 of the expected value. Figure 5 presents similar data for Szechwan earthquakes, for which the observed amplitudes at CHG and QUE are 1.3 times, at NIL 2.0 times and at KBL 0.79 times the expected value for an m_b = 5.0 earthquake.

AMPLITUDES OF Pg WAVES

Figure 6 presents the amplitude data for the vertical component of the Pg ground motion for southern Asia equalized to m_b = 5.0. The solid-line curve has a slope of -3.5, indicating a fairly rapid decrease of amplitude with distance. By comparison, the slope of Pg for Iranian earthquakes recorded in Iran is -5.85 (Nuttli, 1978) at distances of 700 to 1200 km. For the eastern United States Evernden (1967) found a slope of -3.42, almost identical to the -3.5 found for southern Asia in this study. Evernden's Pg amplitude values for the western United States are nearly identical to those found for southern Asia. The Iranian Pg amplitudes are about twice as large at 500 km epicentral distance, and become equal to the western United States and southern Asia at 1000 km. At larger distances the Iranian Pg amplitudes decrease much more rapidly.

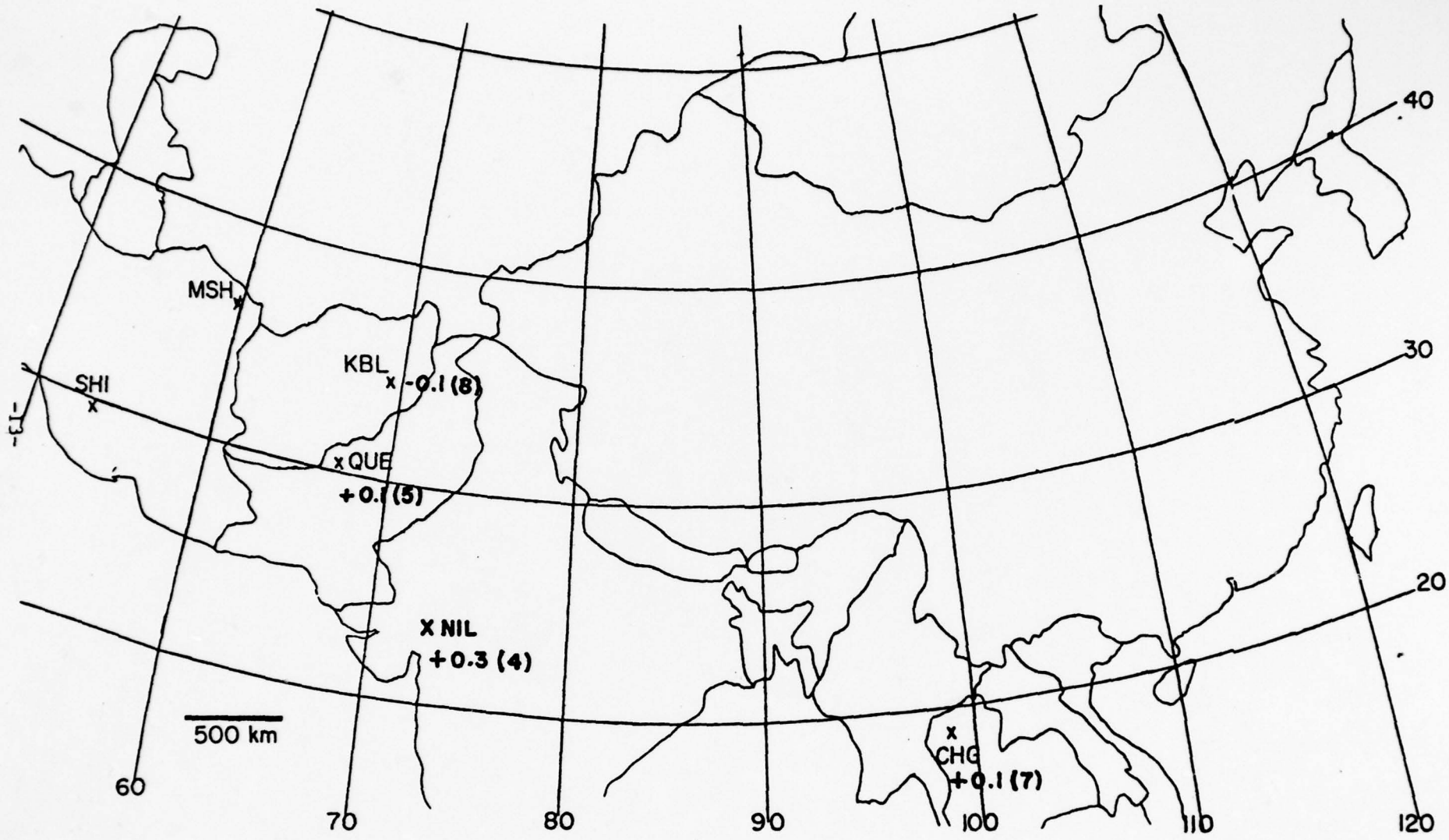

Figure 5. Average P-wave deviations, in m_b units, for earthquakes in Szechwan. The number in parentheses refers to the number of observations.

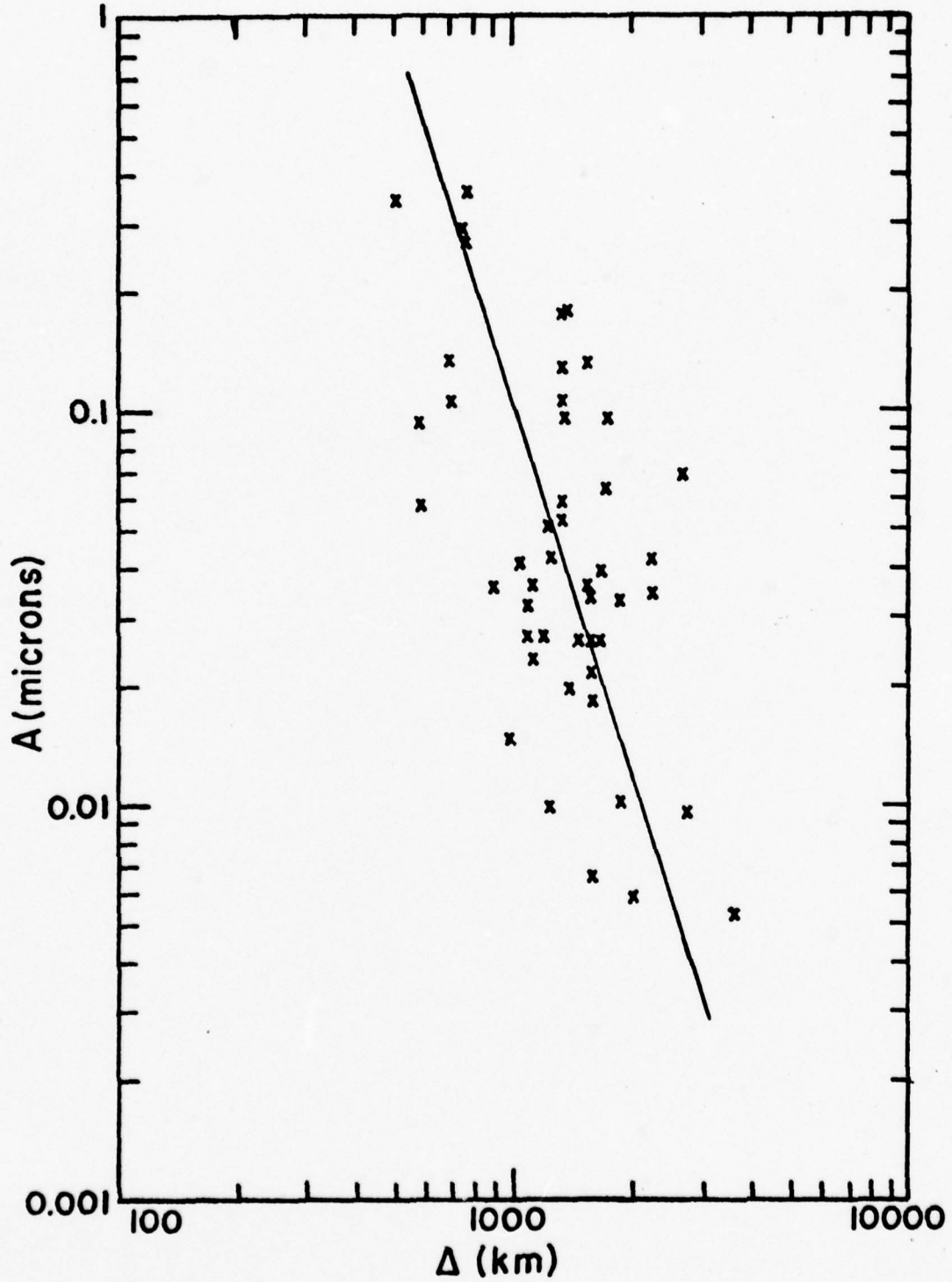

Figure 6. Amplitudes of vertical-component, 1-sec period Pg waves equalized to an m_b = 5.0 earthquake. The straight-line curve has a slope of -3.5.

AMPLITUDES OF Sn WAVES

Figure 7 presents the amplitude data for the horizontal component of 1-sec period Sn waves for southern Asia equalized to m_b = 5.0. At distances of 750 to 900 km the average curve is practically identical to that given by Nuttli (1978) for Iranian earthquakes recorded in Iran. However, at distances beyone 900 km the Iranian curve has a steeper slope, indicating a higher attenuation in Iran at the larger distances. The slope of the southern Asia curve is -3.1, wheras for Iran it was found to be -4.35.

Figure 8 presents the amplitude data for the vertical component of 1-sec period Sn waves for southern Asia equalized to m_b = 5.0 Although one would expect the average curve to have the same slope as for the horizontal Sn data, the slope of the vertical-component curve is smaller, namely -2.2. The differences in slope result principally from differences in amplitude at distances less than 1000 km, for which there are few data points.

AMPLITUDES OF Lg WAVES

Figure 9 presents attenuation curves for the vertical component of 1-sec period Lg waves for an m_b = 5.0 earthquake. The parameter is the absorption coefficient, which is allowed to vary from 0.015 km^{-1} to 0.0006 km^{-1}, a range which spans the observed values for short period (0.1 to !.0 sec) Lg waves in various geological regions. If extended back to 1 km all of the curves would indicate a ground amplitude of 800 microns, which can be considered as the near-field

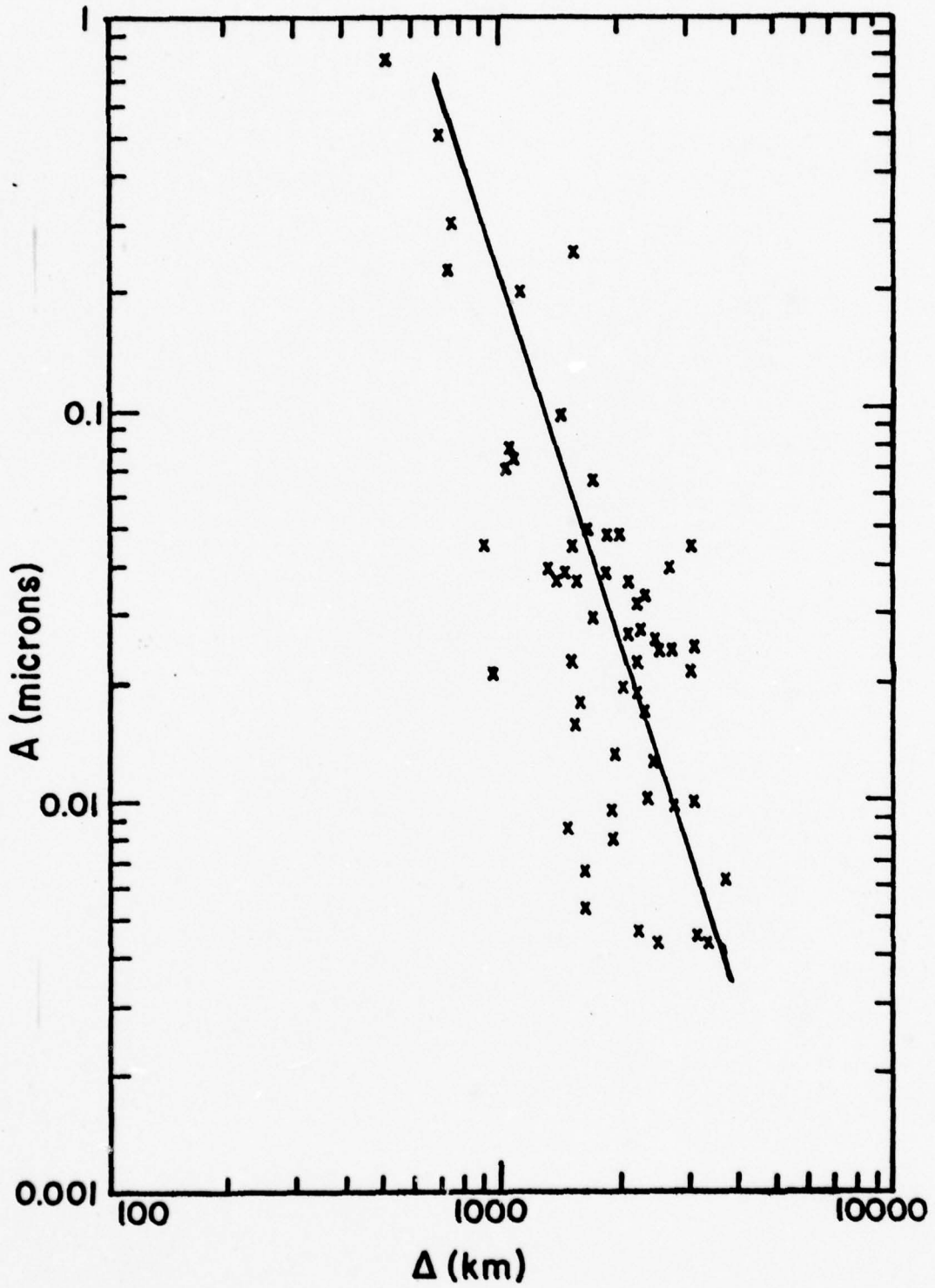

Figure 7. Amplitudes of horizontal-component, 1-sec period Sn waves equalized to an m_b = 5.0 earthquake. The straight-line curve has a slope of -3.1.

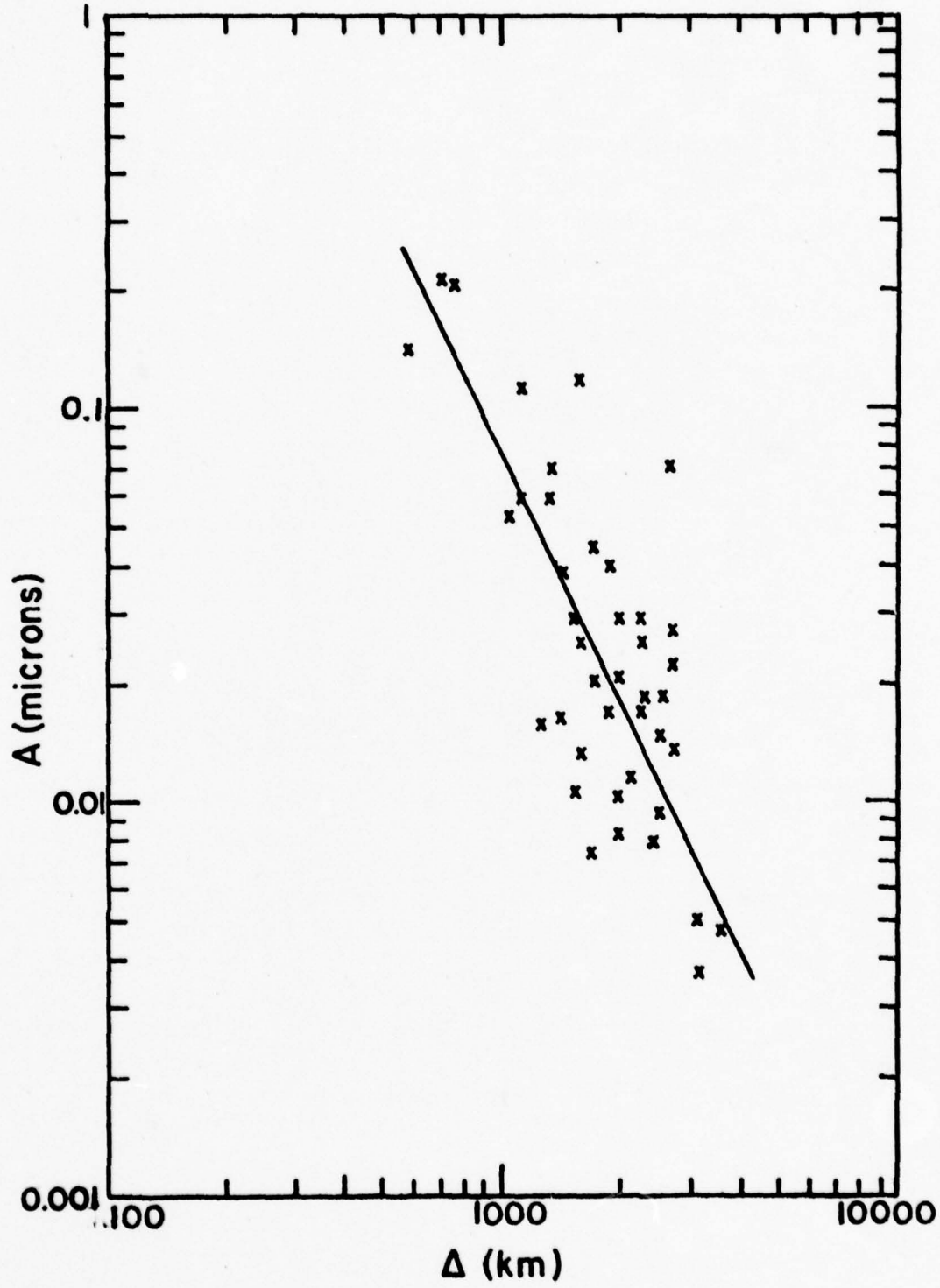

Figure 8. Amplitudes of vertical-component, 1-sec period Sn waves equalized to an m_b = 5.0 earthquake. The straight-line curve has a slope of -2.2.

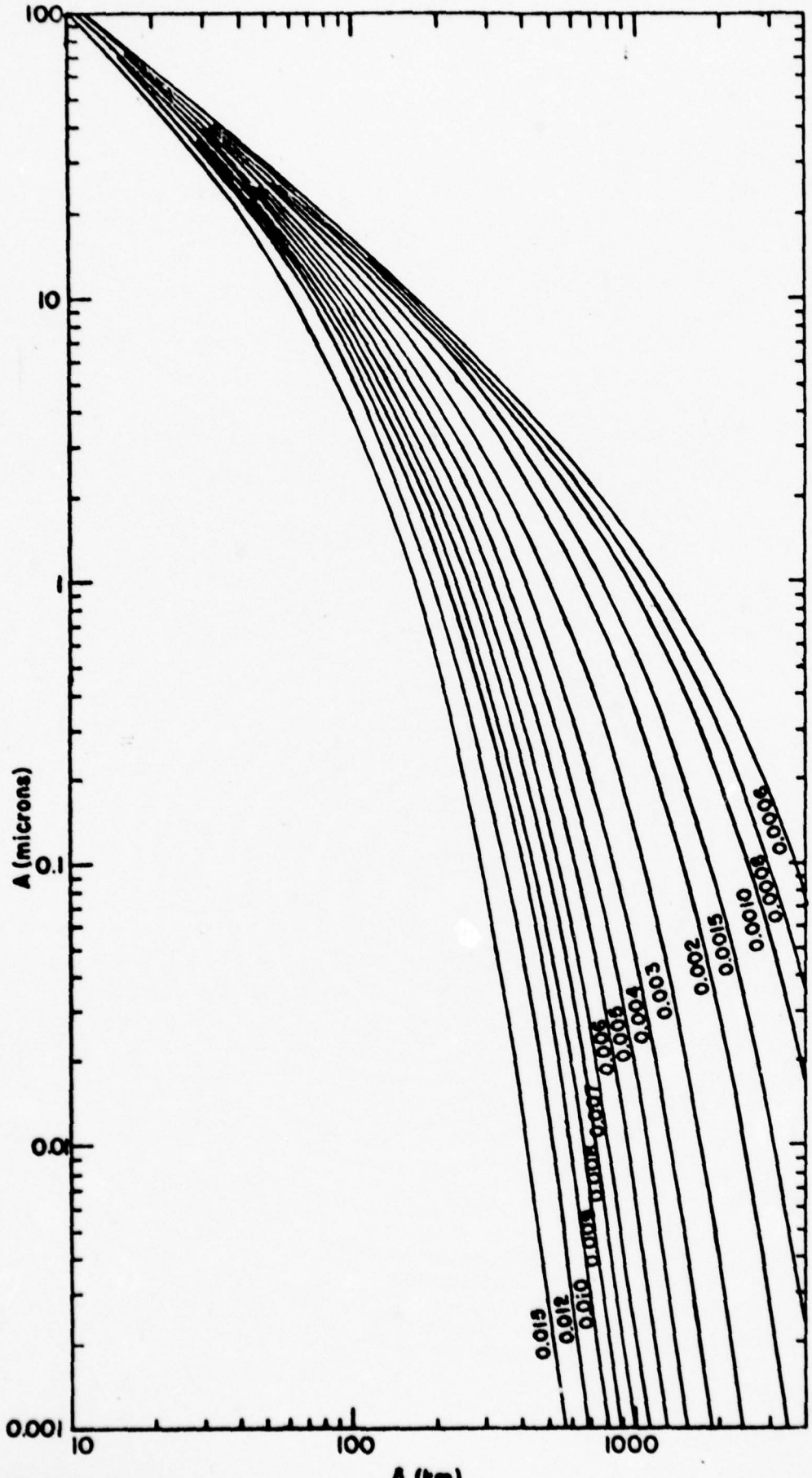

Fig. 9. Time-domain attenuation curves for 1-sec Lg waves for an m_b= 5.0 earthquake.

or source extrapolation of the far-field data. In practice, however, the curves should not be used at distances less than about 50 km to estimate ground motion, because 1-sec period Lg waves may not completely develop at shorter epicentral distances. The curves of Figure 8 satisfy the relation

$$A(\Delta) = 2.0855\ (\sin \Delta)^{-\frac{1}{2}}\ (\Delta)^{-1/3}\ \exp(-\gamma \Delta)$$

where A is in microns and Δ is in radians, except that it is customary to express Δ in the exponent in kilometers, and correspondingly γ in km^{-1}. The number 2.0855 was chosen to satisfy the far-field data of Lg-wave amplitudes in both northeastern America and in Iran, where the far-field data in each case extrapolate back to a value of 800 microns at 1 km epicentral distance.

Figure 9 was used to estimate the average value of the Lg absorption coefficient for the path between a specific epicenter and a specific station. The amplitude, equalized to an $m_b = 5.0$ earthquake, was plotted as a function of epicentral distance on Figure 9, and the appropriate value of the coefficient of absorption was read from the curves. The results of such analysis are shown in Figure 10. From that figure it can be seen that the largest values for the coefficient of absorption occur for paths between western Tibet and KBL, QUE, and NIL. The lowest values of absorption occur for paths from eastern Tibet and northeastern India to NIL, KOD and KBL. By way of comparison, the average value of the absorption coefficient for 1-sec Lg waves in Iran was 0.0045 km^{-1} (Nuttli, 1978). Absorption for paths across the Indian shield is low, but greater (0.0015 to 0.0020 km^{-1}) than for northeastern America (0.0006 km^{-1}). Surprisingly, paths from eastern Tibet and Szechuan across the

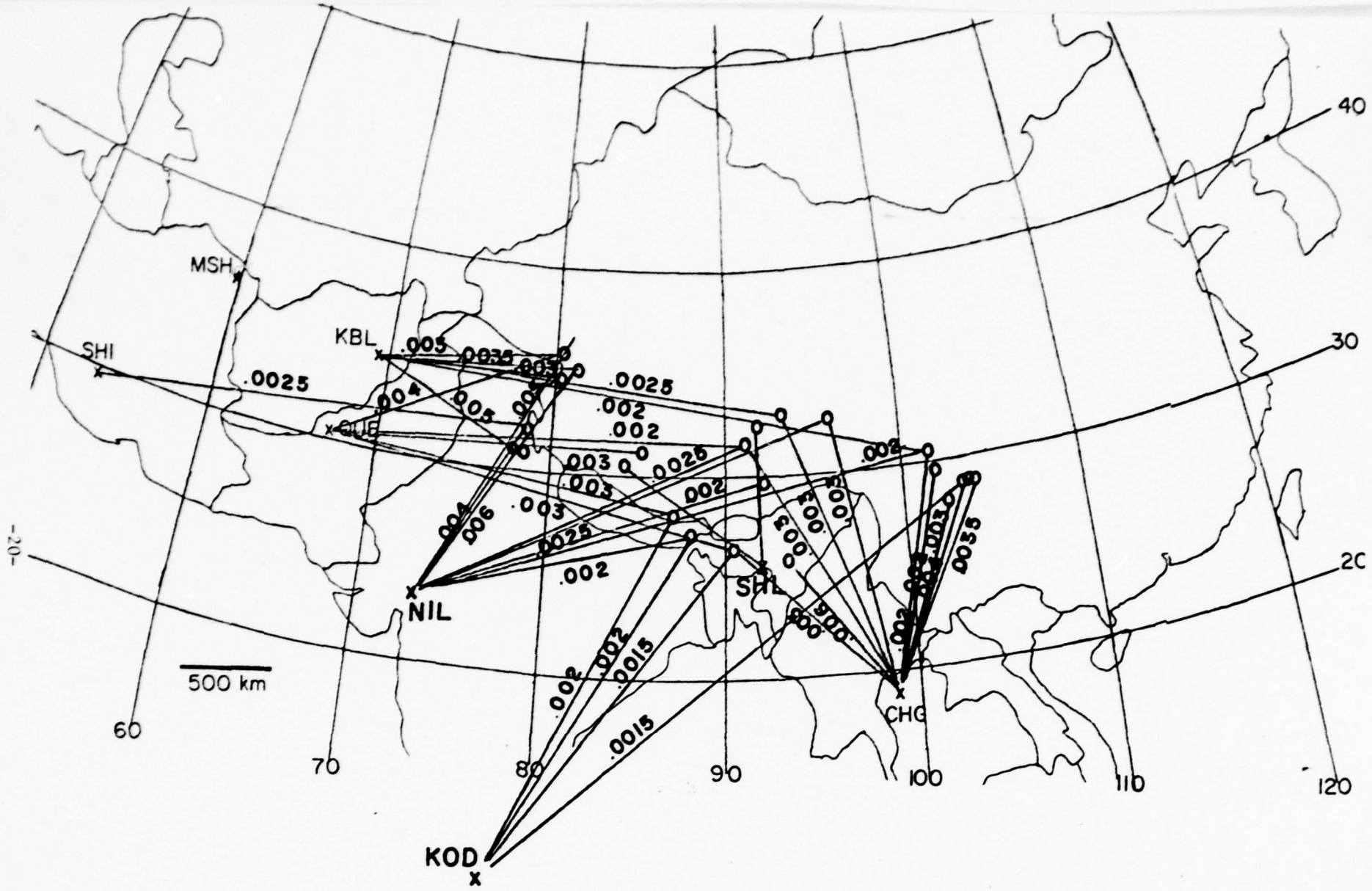

Figure 10. Average values of absorption coefficient, in km^{-1}, for vertical-component, 1-sec period Lg waves. The circles represent the epicenters.

Himalayas to NIL show relatively small values for the absorption coefficient, namely 0.0020 to 0.0025 km^{-1}, which is significantly lower than that observed for Iran and for the western United States.

Figure 11 presents the vertical-component Lg amplitudes for all the paths in southern Asia. The solid-line curve is a theoretical curve with absorption coefficient equal to 0.0025 km^{-1}. If the curve is extrapolated back to 1 km it gives an amplitude of 800 microns, similar to that found for Iran and northeastern America. Thus it appears that the source excitation of 1-sec Lg waves is independent of source region for earthquakes with foci in the crust, i.e., if their m_b's as determined by teleseismic P waves are equal, their extrapolated Lg amplitudes at 1 km epicentral distance will be equal.

AMPLITUDE OF CRUSTAL PHASES AS A FUNCTION OF EPICENTRAL DISTANCE

For the determination of the detection capability of a seismograph network it is necessary to know which seismic phases will have the largest amplitude at a specific epicentral distance. Figure 12 presents this information in graphical form, by means of stick seismograms. In the figure the amplitudes of the vertical component of P, Pg, Sn and Lg are plotted on a linear amplitude scale for distances of 500, 1000 and 2000 km. At 500 km distance in southern Asia Pg is the largest amplitude phase, and Lg is also comparatively large. P and Sn are small, of the order of 0.1 microns. (For an m_b = 4.0 event, P and Sn would have amplitudes of about 10 millimicrons

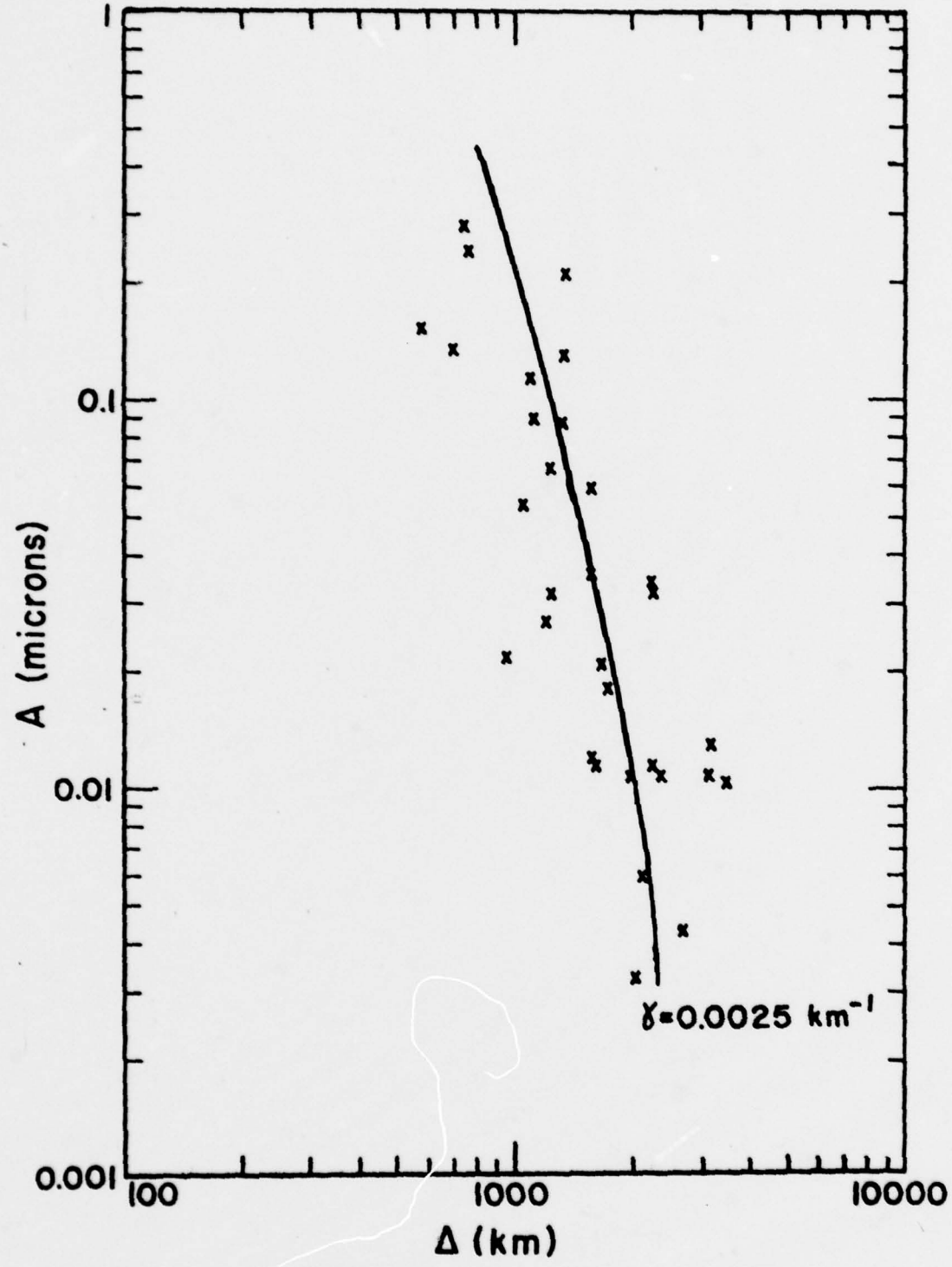

Figure 11. Amplitude data for vertical-component, 1-sec period Lg waves equalized to an m_b = 5.0 earthquake. The solid-line curve is a theoretical surface-wave attenuation curve in the time domain for an absorption coefficient of 0.0025 km^{-1}.

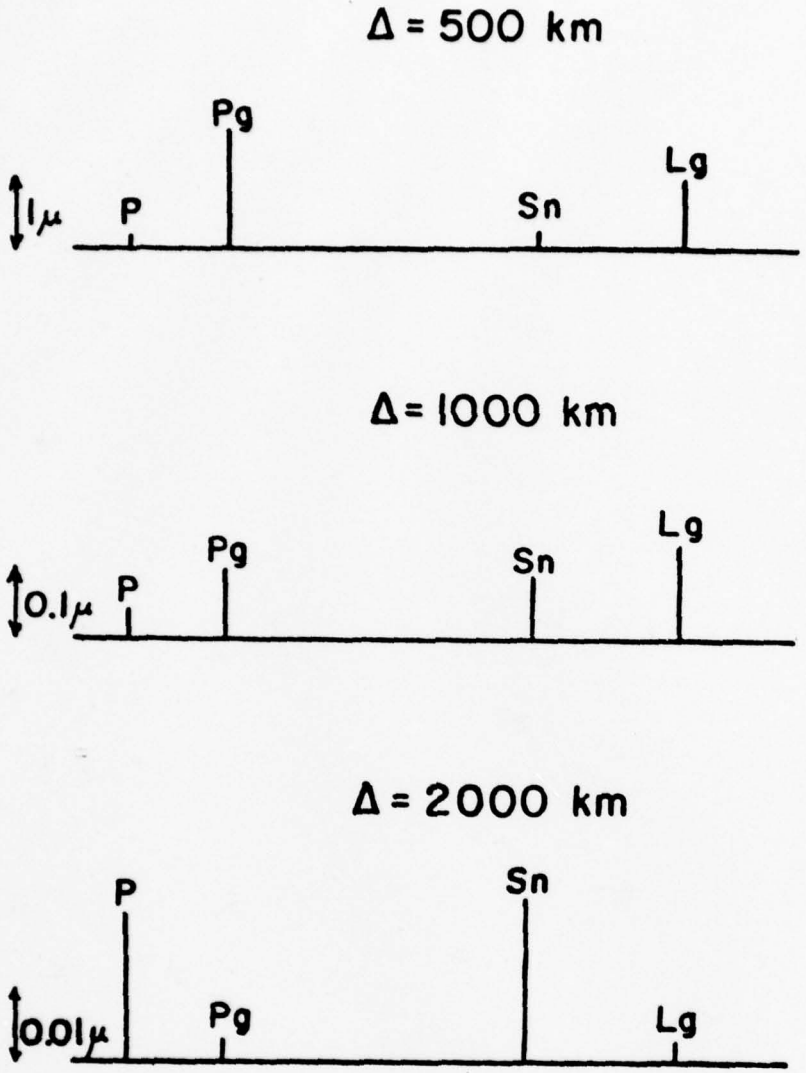

Figure 12. Stick seismograms showing the amplitudes of the vertical-component, 1-sec period ground motionfor the crustal phases in southern Asia.

at 500 km distance.) At 1000 km all four phases have about equal amplitudes, of the order of 100 millimicrons for an m_b = 5.0 event. At 2000 km distance the effects of absorption on Pg and Sg are severe, so that their amplitudes are only about one-tenth those of P and Sn.

In summary, Pg and Lg have the potential for detecting smaller events than P and Sn can detect for distances up to about 1000 km, but at the larger distances the phases P and Sn provide the best detection. For location of events, P (or Pn) is always the best phase to use, because it is the only phase with a sharp onset whose arrival time can be measured to a tenth of a second.

COMPARISON TO AMPLITUDES OF CRUSTAL PHASES RECORDED IN CENTRAL ASIA

Antonova et al (1978) gave spectral amplitude data for earthquakes in four source regions recorded at the station Talgar, which is near Alma Ata in southeastern Kazakh, central Asia. From their Figures 18, 20, 22 and 23, which are attenuation curves for amplitude-to-period ratios of P, Pg, S and Lg for frequencies of 0.35 to 11 Hz, equalized to a magnitude 5.0 event, one can construct stick seismograms similar to those of Figure 12. Figure 13 shows such seismograms for 1-Hz waves for earthquake source regions to the northeast, to the east, to the south and to the west of Talgar. In general at distances of 500 and 1000 km the seismograms are similar in amplitude and character to those recorded in southern Asia, except that the Lg waves for earthquakes to the northeast of Talgar (epicenters

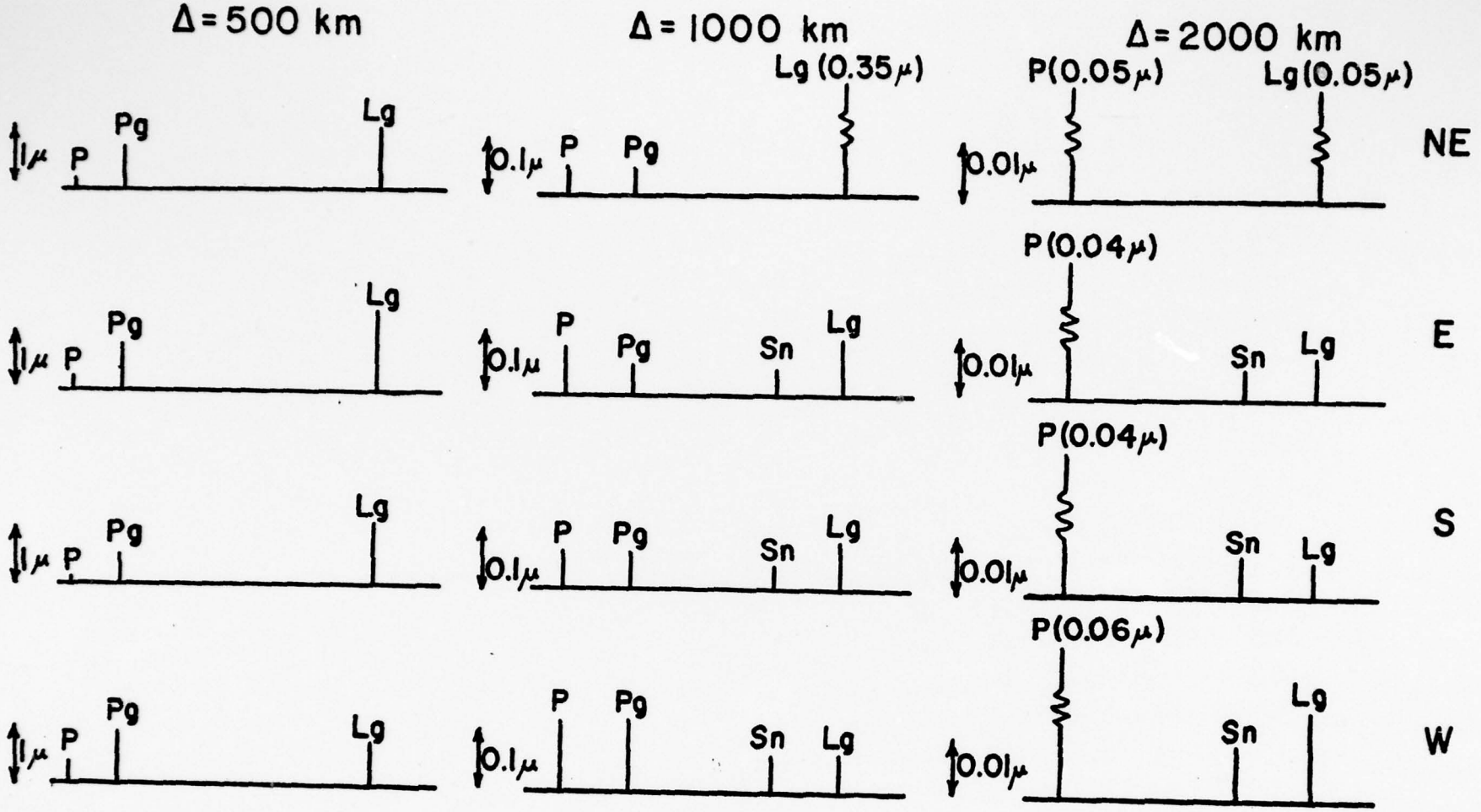

Figure 13. Stick seismograms showing the amplitudes of the vertical-component, 1-sec period ground motion for the crustal phases recorded at the seismograph station Talgar in central Asia. The earthquake source regions are to the northeast, east, south and west of Talgar.

in Zaysan, Altag, Sayan, Pribay kalye and Trans-Baykal) are much larger, of the character of what one would expect for paths crossing a shield region, even though the region in question would be classified as tectonic rather than shield. At 2000 km the P waves for all four directions to Talgar are two to three times larger than for southern Asia, and again for earthquakes to the northeast the Lg amplitudes are about two orders of magnitude greater than those observed for southern Asia. Even for sources to the east (northeast China and Mongolia), to the south (Pakistan, Nepal and India), and to the west (South Tyan' Shan', Pamir, Tadzhik, Kopet-Dag, Iran and Caucasus) the Lg amplitudes at 2000 km are two to five times those observed in southern Asia. From Figure 9 this would indicate that the coefficient of absorption of 1-sec period Lg waves to the northeast of Talgar is 0.0006 km^{-1} (similar to that of eastern North America), to the east is 0.0015 km^{-1}, to the south is 0.002 km^{-1} and to the west is 0.0012 km^{-1}.

CONCLUSIONS

In general, crustal phases propagating across southern Asia are attenuated more than in eastern North America and in central Asia, but less than in the western United States and in Iran. Only in northern India, northern Pakistan and Afghanistan is the attenuation as severe as it is in the western United States and Iran.

P (or Pn) is the best-suited wave to locate earthquakes in southern Asia, because it is the only crustal phase with a sharp onset. It will have amplitudes of at least one millimicron to

distances as large as 3500 km for an m_b = 4.0 event. For detection purposes, Pg and Lg will have larger amplitudes than P for distances to 1000 km. Beyond 1000 km P and Sn have the largest amplitudes.

The P amplitudes for southern Asian earthquakes depart by as much as 0.5 m_b units or greater from the Gutenberg-Richter (1956) amplitudes at distances of 500 to 2500 km. Thus at these distances the Gutenberg-Richter calibration function should not be used to determine m_b of southern Asia earthquakes. The nuclear explosion data given by Nuttli (1971) provide a close fit to the southern Asia data, but unfortunately the explosion data curve only begins at 2200 km distance.

From data given by Antonova et al (1978) the attenuation of 1-sec period Lg waves for earthquakes in Baykal recorded at Talgar (43^{o}N, 78^{o}E) is similar to that in eastern North America, even though the former is for a path across a tectonic region just north of Mongolia. If a broad generalization can be made from this one data set, one might expect that similar small values of Lg attenuation would be found in the Russian platform and the non-tectonic Siberian interior. Thus Lg could well have the potential for detecting events of magnitude even less than 4 out to distances of 2000 km in the interior of the USSR, although Lg could not be used to accurately locate such events.

REFERENCES

Antonova, L.V., F.F. Apticaev, R.J. Curochkina, I.L. Nersesov, A.V. Nikolaev, A.I. Ruzaykin, E.N. Sedova, A.V. Sitnikov, F.S. Tregub, L.D. Fedorscaya and V.I. Halturin (1978). Experimental Science Studies of the Earth's Interior, Institute of Earth Physics, USSR Academy of Sciences, Nauka, Moscow.

Evernden, J.F. (1967). "Magnitude determination at regional and near-regional distances in the United States," Bull. Seis. Soc. Am., 57, 591-639.

Gutenberg, B. and C.F. Richter (1956). "Magnitude and energy of earthquakes," Ann. Geofis. (Rome), 9, 1-15.

Nuttli, O.W. (1971). "The amplitudes of teleseismic P waves," Bull. Seism. Soc. Am., 61, 343-356.

Nuttli, O.W. (1973). "Seismic wave attenuation and magnitude relations for eastern North America," Jour. Geoph. Res., 78, 876-885.

Nuttli, O.W. (1978). "Amplitudes and attenuation of seismic crustal phases at regional distances in Iran" in Research in Seismology, Final Report by B.J. Mitchell and O.W. Nuttli, ARPA Contract F44620-73-C-0042, Nov. 1978, 12-31.

Determination of Q models from Surface Wave Spectra

by

Chiung-chuan Cheng

The determination of Q structure from surface wave spectra of a single seismogram (our previous reports) requires the source mechanism as well as the focal depth be known. These are not always known as precisely as we would like. However, Tsai and Aki (1970) investigated variations of the surface wave amplitude spectrum which were due to uncertainties of these factors and concluded that effects caused by factors other than the focal depth were relatively small. We have made further comparisons between the nature of spectral variations caused by varying focal depth and that by varying Q structures.

A stochastic inversion scheme is applied to obtain Q from surface wave spectra.

The effect of focal depth and Q structure on surface wave spectra

The Rayleigh or Love wave spectral amplitude of a certain mode at a certain period is assumed to be

$$y = y_o e^{-\gamma R} \tag{1}$$

where y_o is computed amplitude without attenuation.

The effect of focal depth is present in y_o through a multiplication factor, the excitation coefficient, which in turn is the source spectral amplitude multiplied by a very complicated function of the focal depth and the source mechanism.

The wave amplitude decreases exponentially with the product of the attenuation coefficient γ and the epicentral distance R. For a layered earth model, the Rayleigh wave attenuation coefficient is related to the compressional- and shear-wave velocities, α and β, and the associated quality factors, Q_α and Q_β (Anderson et al., 1965; Mitchell, 1975).

$$\gamma = \frac{\pi}{T}\left[\sum_{\ell=1}^{N}\left(\frac{\alpha_\ell}{C^2}\frac{\partial C}{\partial \alpha_\ell}\right)\omega\rho\beta\ Q_{\alpha\ell}^{-1} + \sum_{\ell=1}^{N}\left(\frac{\beta_\ell}{C^2}\frac{\partial C}{\partial \beta_\ell}\right)\omega\rho\alpha\ Q_{\beta\ell}^{-1}\right] \tag{2}$$

The complexity of the way surface wave spectrum varies with the focal depth is illustrated in figures 1 and 2. The contours show the values of log y. The source is assumed to be a 45^o thrust fault having a seismic moment of 1.0×10^{24} dyne-cm. The epicentral distance is 1000 km, and the station is located at an azimuth of 45^o from the source. A Q model which has Q_β values of 250 from the surface to a depth of 17 km, 2000 at all greater depths, and a Q_α being twice Q_β everywhere

(Herrmann and Mitchell, 1975) is used. Figure 1 shows the result of the fundamental mode, and figure 2 the first higher mode Rayleigh wave. The general feature shows that the energy lobes migrate to the longer periods as the focal depth increases. Nevertheless, their relative heights vary.

Figure 3 shows the effect of varying the Q values in the upper layer. The same source is assumed and is fixed at a depth of 10 km. The contours show log y for the fundamental mode Rayleigh wave. From equation (1), it is seen that log y is a function linear in the varying Q values. A straight line drawn for constant period in the figure will intersect the contours with equi-intervals, showing a constant slope for log y to decrease with increasing Q_β^{-1}.

Stochastic inversion of surface wave spectra

An observed spectral amplitude z is in general different from the theoretical amplitude y computed from equation (1), with presumed seismic moment and Q model. To fit y and z, the seismic moment and Q model have to be adjusted.

Assuming that Q_α values are twice that of Q_β everywhere, from equations (1) and (2),

$$\frac{R\pi}{T} \sum_{\ell=1}^{N} \left[\tfrac{1}{2}\left(\frac{\alpha_\ell}{C^2} \frac{\partial C}{\partial \alpha_\ell} \right) \omega\rho\beta + \left(\frac{\beta_\ell}{C^2} \frac{\partial C}{\partial \beta_\ell} \right) \omega\rho\beta \right] \Delta Q_{\beta\ell}^{-1} + RC$$

$$= \ell n\, y - \ell n\, z$$

where $\Delta Q_{\beta\ell}^{-1}$ is the adjustment for $Q_{\beta\ell}^{-1}$ in each layer of the model, and the seismic moment is adjusted to by multiplied by exp (-RC).

Fitting y and z over all the periods and modes of available data points yields a system of equations, which can be written as

$$Ax = b$$

where x is the vector to be solved,

$$x = (\Delta Q_{\beta 1}, \Delta Q_{\beta 2}, \Delta Q_{\beta 3}, \ldots \Delta Q_{\beta N}, C)^T.$$

With the transformations (Wiggins, 1972) that

$$A' = S^{-\frac{1}{2}} A W^{\frac{1}{2}}$$

$$x' = W^{-\frac{1}{2}} x$$

$$b' = S^{-\frac{1}{2}} b$$

the matrix equation can be rewritten as

$$A'x' = b'$$

W and S are assumed to be diagonal matrices. The stochastic inversion is applied to solve for x'.

$$x' = (A'^T A' + \sigma^2 I)^{-1} A'^T b'$$

Thus,

$$x = (W^{\frac{1}{2}} A^T S^{-1} A + \sigma^2 I)^{-1} W^{-\frac{1}{2}} A^T S^{-1} b \qquad (3)$$

This inversion scheme yields an estimate of x that minimizes

$$\begin{aligned} \varepsilon^2 &= (A'x' - b')^T (A'x' - b') + \sigma^2 x'^T x' \\ &= (S^{-\frac{1}{2}} Ax - S^{-\frac{1}{2}} b)^T (S^{-\frac{1}{2}} Ax - S^{-\frac{1}{2}} b) + \\ &\quad \sigma^2 (W^{-\frac{1}{2}} x)^T (W^{-\frac{1}{2}} x) \end{aligned}$$

The introduction of S enables us to add weights to the observations. The combination of σ^2 and W provides a measure of how freely each of the parameters can deviate from its presumed value.

Spectral comparison for vertical component Rayleigh waves from the southeastern Missouri earthquake of October 21, 1965 (Mitchell, 1973;

Herrmann, 1974) recorded at MDS was made with a two-layer Q model (our previous report). A discrepancy could be noticed for the fundamental mode spectrum at short periods (figure 4), so the observed data set has been inverted using equation (3) in a hope to improve the fit. The starting Q model is the same as the one used in spectral comparisons before. However, the upper layer, which was 17 km thick and had Q_β values of 250, is divided into a layer of 7 km overlying another of 10 km; and a layer of 50 km is added to the top of the half-space, which had a Q_β of 2000.

The resulting model is shown in table 1. A comparison of observed and theoretical spectra appears in figure 5.

Discussion

The way in which the surface wave spectrum varies with the focal depth is different from the way it varies with the Q model, and is much more complicated. Attempts to invert surface wave spectra to obtain the focal depth and Q model simultaneously is impractical compared to that to obtain the Q model only, because of its non-linearity and large computer time consumption. Even if the focal depth is not well determined in advance, the Q model can still be obtained by inverting with several presumed focal depths. An adequate fit between the theoretical and observational spectra occurs with the proper focal depth. Analyses of several sets of spectral data using this method are in progress.

References

Anderson, D.L., A. Ben-Menahem and C.B. Archambeau, Attenuation of seismic energy in the upper mantle, J. Geophys. Res., 70, 1441-1448, 1965.

Herrmann, R.B., Surface wave generation by central United States earthquakes, Ph.D. Dissertation, Saint Louis Univ., 1974.

Herrmann, R.B. and B.J. Mitchell, Statistical analysis and interpretation of surface-wave anelastic attenuation data for the stable interior of North America, Bull. Seism. Soc. Am., 65, 1115-1128, 1975.

Mitchell, B.J., Radiation and attenuation of Rayleigh waves from the southeastern Missouri earthquake of October 21, 1965, J. Geophys. Res., 78, 886-899, 1973.

Tsai, Y.B. and K. Aki, Precise focal depth determination from amplitude spectra of surface waves, J. Geophys. Res., 75, 5729-5743, 1970.

Wiggins, R.A., The general linear inverse problem: implication of surface waves and free oscillations for earth structure, Rev. Geophys. Space Phys., 10, 251-285, 1972.

Table 1. Inversion of MDS data

	Starting Model	Result Model
$Q_{\beta 1}$	250	158
$Q_{\beta 2}$	250	260
$Q_{\beta 3}$	2000	2761
$Q_{\beta 4}$	2000	15
C	0	0.000344

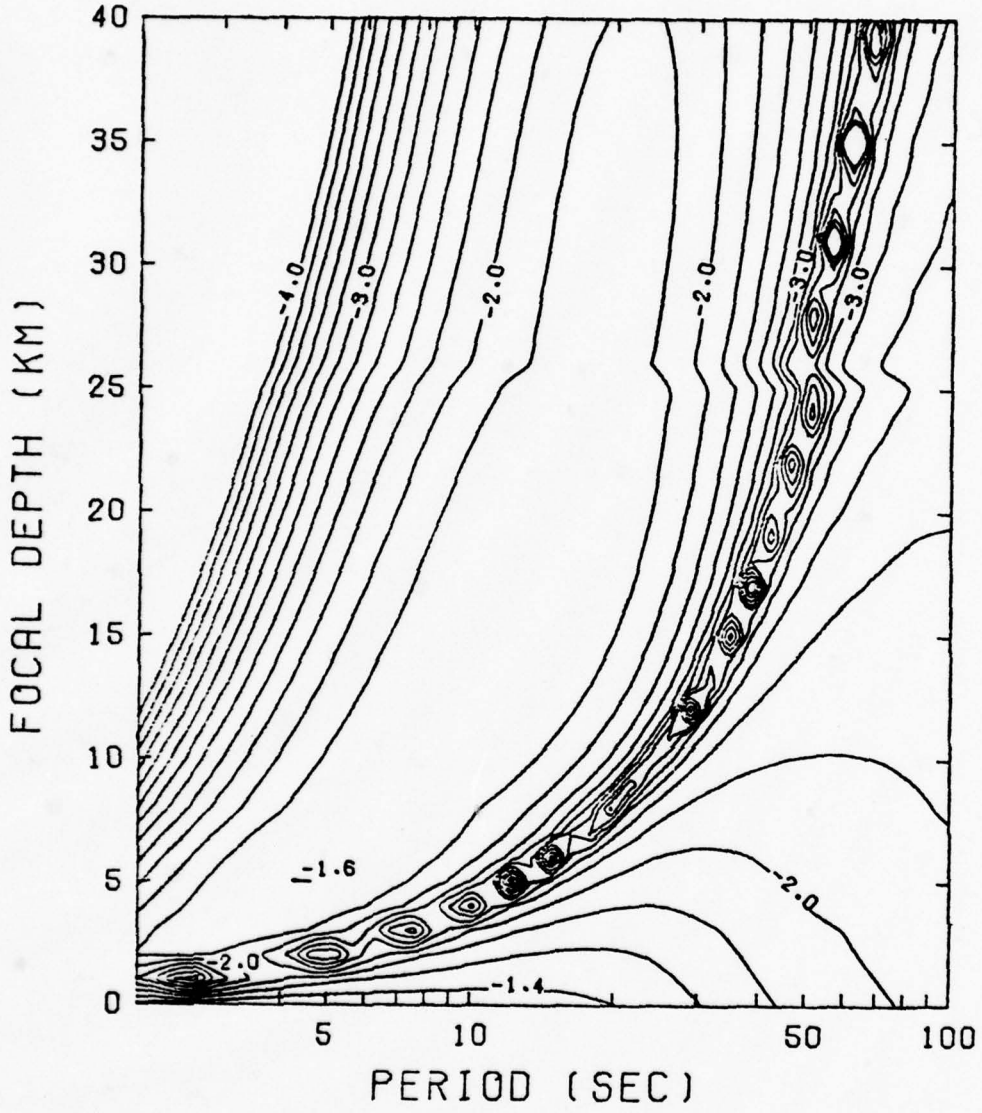

Figure 1. Contours showing the fundamental mode Rayleigh wave logarithmic spectrum for various focal depths.

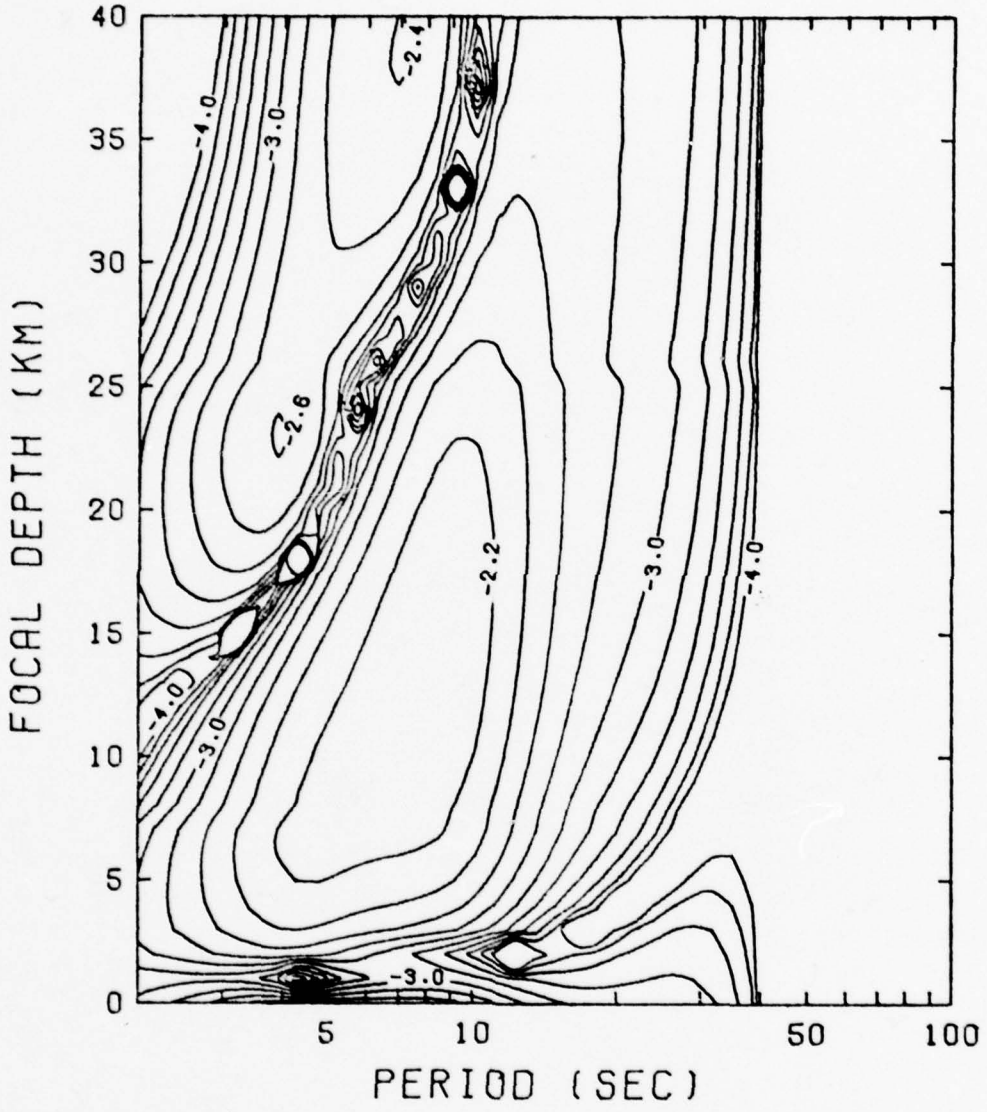

Figure 2. Contours showing the first higher mode Rayleigh wave logarithmic spectrum for various focal depths.

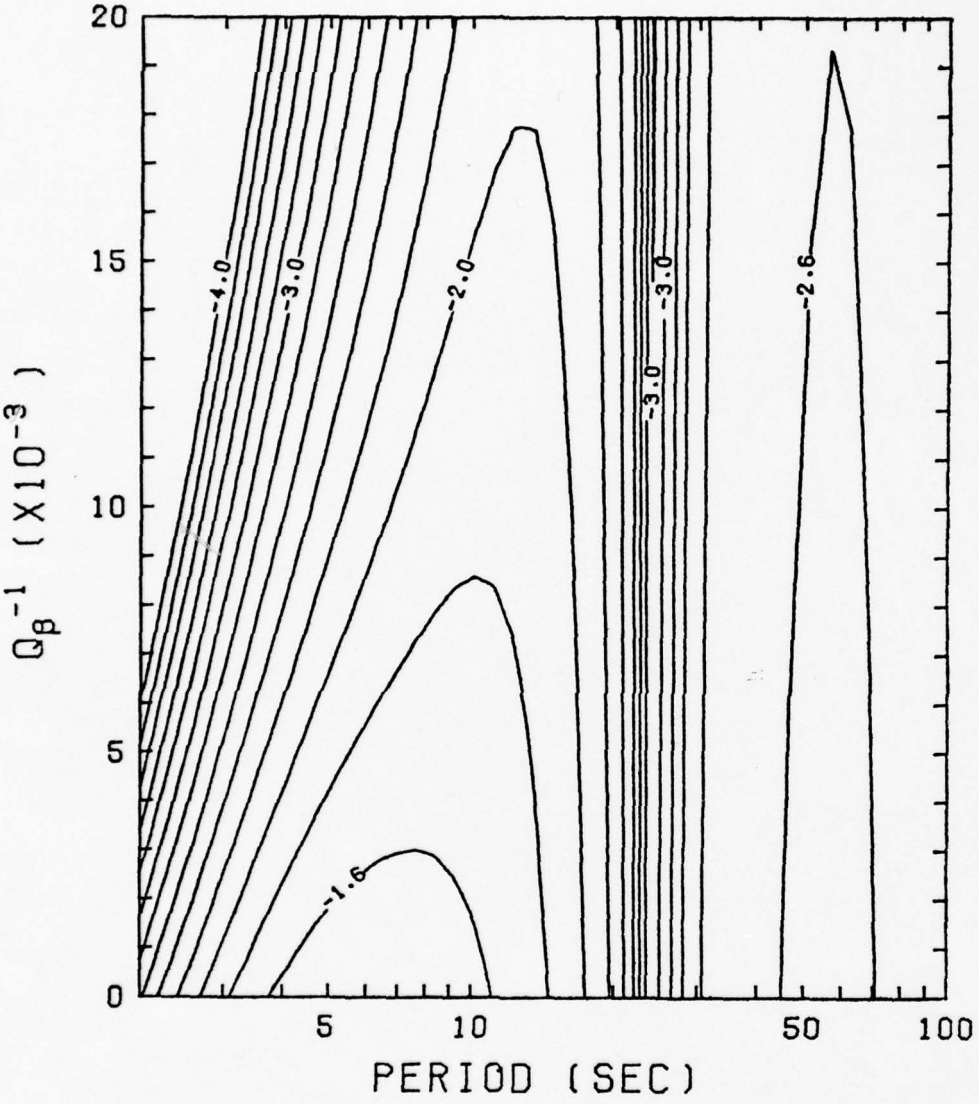

Figure 3. Contours for the fundamental mode Rayleigh wave logarithmic spectrum attenuated with a two-layer model which has various Q_β values in the upper layer.

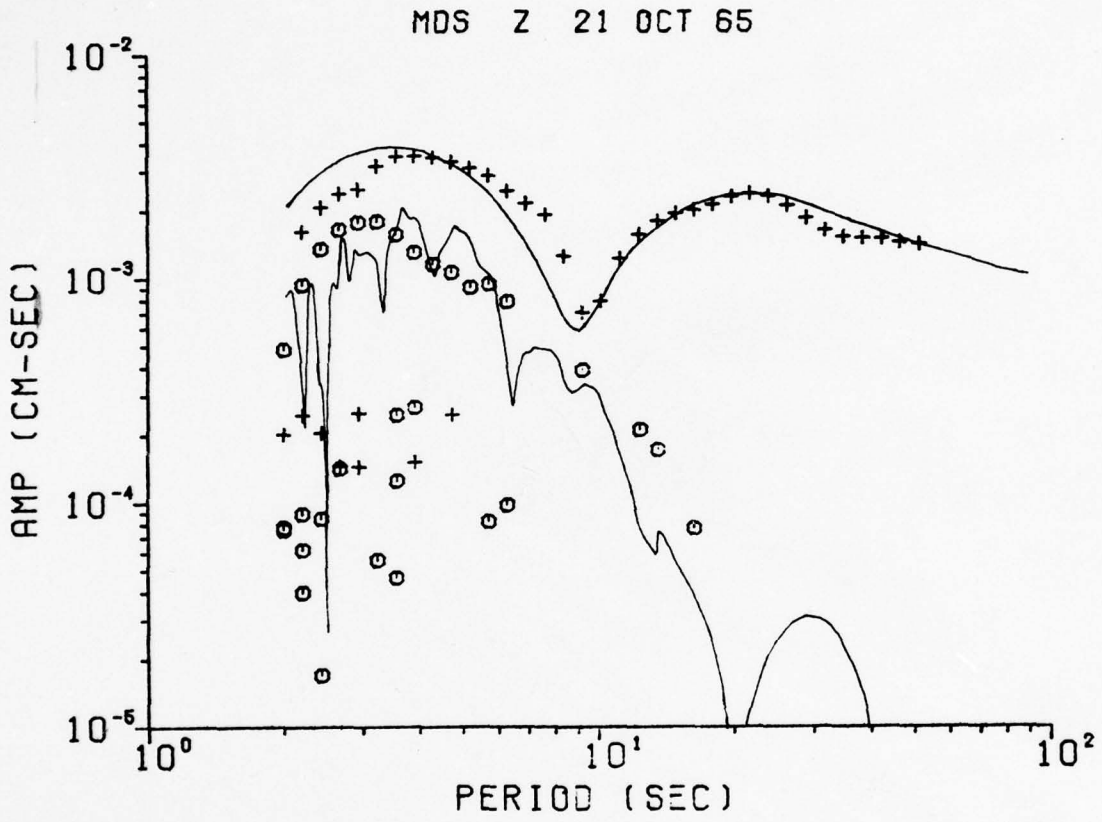

Figure 4. Comparison of theoretical and observational amplitude spectra, based on a two-layer Q model.

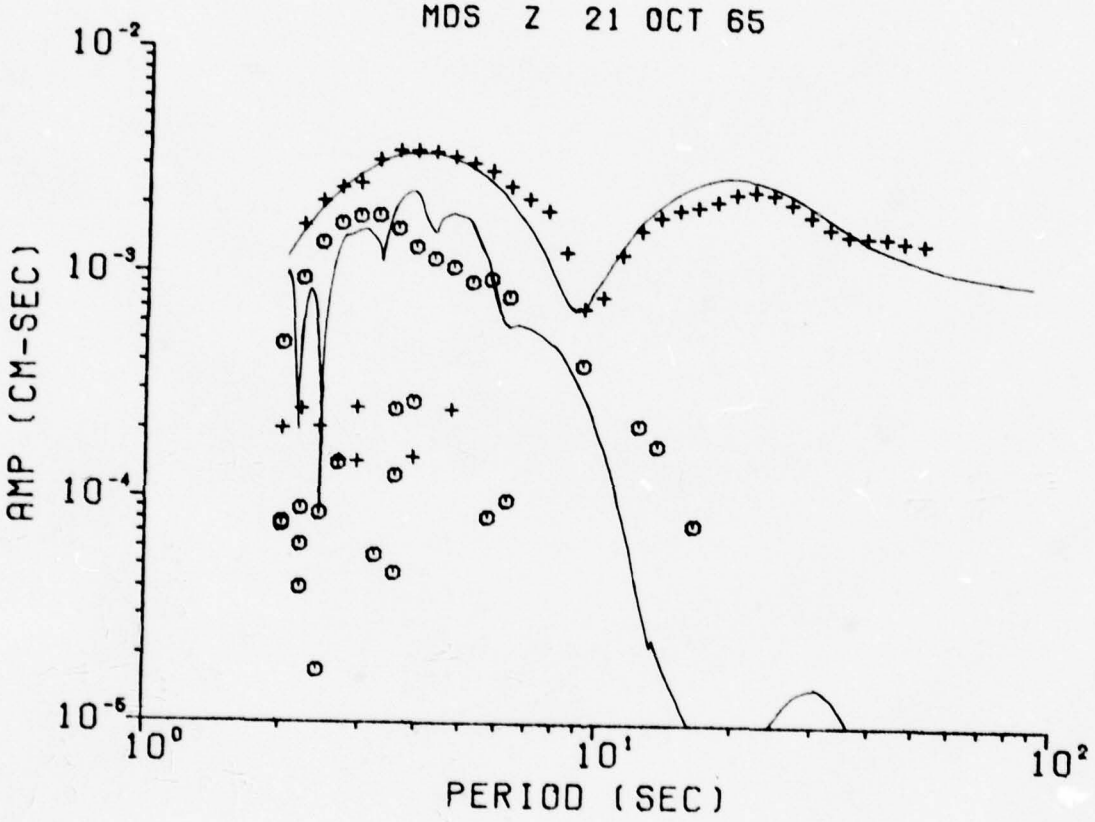

Figure 5. Comparison of theoretical and observational amplitude spectra, based on the four-layer Q model obtained from inversion.

Source Studies of Some Eurasian Earthquakes

by

Hui-Yuin Wen Wang

In the last semi-annual report, we mentioned that in order to know the source time functions of the earthquakes, several determinations should be made for comparing synthetic seismograms with observed ones: (1) source velocity model; (2) receiver velocity model; (3) seismic wave attenuation data; (4) fault plane solution; (5) focal depth; (6) seismic moment. Especially the seismic velocity model and attenuation coefficients are the two most important effects on synthetic seismograms. In this study, surface waves generated by 22 earthquakes which occurred in the Tibetan Plateau and/or on the Tibetan border were used to analyze the crustal structure across Tibet.

Geologic, sesimic, and gravity data imply that the current tectonic activity in Asia is the consequence of continental collision between India and Eurasia. East-west trending strike-slip faults are most observed in China. Movements on them may allow material lying between the stable portions of the Indian and Eurasian plates to move laterally out of the way of these two plates. The Tibetan Plateau has a unique topographic feature of high altitude, which is not a direct result of the continental collision but of uplift during northerly underthrusting of the Indian subcontinent along the deep crustal fracture. This led to an approximate doubling of crustal thickness under the Tibetan Plateau (Molnar & Tapponmier, 1975; Powell & Conaghan,

1973). Santo (1965), Gupta & Naraub (1967), Chen & Molnar (1975), and Chun & Yoshii (1977) analyzed the dispersion of the fundamental Rayleigh waves and found that the crustal thickness in Tibet was 65 to 70 km.

Table 1 gives the events which are used in the study. The paths of use in the construction of the Tibetan velocity model are obtained by selecting those which are largely confined to the Tibetan region. Therefore, the surface waves to stations as KBL, QUE, NIL, NDI, and SHL have been digitized and proceed by the multiple-filter method (Dziewonski et al., 1969). Thirty paths are analyzed to obtain the group velocities of fundamental-mode Rayleigh waves in the 6-60 second period range. The averaged values and standard deviations are given in Table 2. The crustal structure was perturbed by trial and error until the theoretical dispersion curve best matched the observed data. First, we tried Chun & Yoshii (1977)'s TP-4 model. Their curve (triangular sign in Figure 1) is a quite good fit to our data (solid line) for periods smaller than 30 seconds, whereas the group velocities are relatively lower at longer periods. Also TP-4 possesses a trough which is somewhat broader and shifted in period when compared with our data, which have a minimum value centered at 30 seconds. Chun & Yoshii's model is characterized by a crust of about 70 km in thickness with low shear velocities and the upper mantle velocity is low with shear velocity of about 4.45 km/sec. The parameters of the TP-4 model are given in Table 3. By increasing the shear velocity of the lower crust to 3.81 km/sec (named model A in Table 3), this new model indicated by crosses in Figure 1 shows the best fit to the observed data at longer periods. It tends to possess slightly lower velocity values for periods smaller than 30 seconds, the largest

difference being 0.02 km/sec. Such differences are negligible and cannot be resolved within the accuracy limits of the observed data.

Because the seismic stations we chose are near to the Tibetan region, the structure complexities may not affect the surface waves greatly. It is not unreasonable to use the same velocity model for the receiver crust and upper mantle structure.

Determination of attenuation coefficients for paths across Eurasia is very difficult because the paths between sources and stations usually cross more than one tectonic province. Yacoub & Mitchell (1977) divided Eurasia into two regions, one considered to be relatively stable and the other considered to be tectonic in nature. By employing Mitchell's method (1975) to fit observed to theoretical amplitudes by least squares for determining Rayleigh-wave fundamental-mode attenuation coefficients, Yacoub & Mitchell (1977) tested four Eurasian earthquakes and found that the tectonic regions exhibit higher attenuation than the stable regions in the period range below about 20 sec, whereas in the period range above 20 sec, no clear difference can be observed for the two regions. We can take their tectonic attenuation data and apply inversion theory (Backus & Gilbert, 1970) to obtain models of Q_β^{-1} as a function of depth beneath Tibetan region. After Q_β^{-1} models are available, theoretical surface wave attenuation coefficient values for all modes can be computed by using the formula of Anderson et al (1965).

The collection of 70 mm film chips of WWSSN stations at the department is not complete enough to allow us to make fault plane solution and focal depth determination for any one of the Tibetan earthquakes listed in Table 1. Therefore we used ISC data and plotted

the first P-wave motions on a lower focal sphere. The most likely solutions are shown in Figure 2. They are all equivalent to a combination of reverse and strike-slip faulting, with one nodel plane dipping east-west and the other north-south. The T-axis trends southwest.

Discussion

Molner et al. (1973) showed that the strike directions of most earthquakes in Tibet trend either north-south or east-west with a northeast trend of the P-axis. They are normal faulting with an east-west T-axis which may reflect east-west flow of material in the lower crust and upper mantle beneath Tibet to compensate for the pressure imposed by the plate motion. The apparent contradiction we found, that the Tibetan is under compression, may be resolved by observing more data by ourselves. We are planning to make a trip to the National Geophysical Data Center in Boulder in May.

As Figure 1 shows, although the velocity model we computed has a relatively higher group velocity at longer periods as compared with TP-4, the latter data are still within our confidence limits.

References

Anderson, D.L., A. Ben-Menahem, and C.B. Archambeau, Attenuation of seismic energy in the upper mantle, J. Geophys. Res., 70, 1441-1448, 1965.

Backus, G., and F. Gilbert, Uniqueness in the inversion of gross earth data, Phil. Trans. Roy. Soc., London, Ser. A, 266, 123-192, 1970.

Chen, W.P., and P. Molnar, Short-period Rayleigh-wave dispersion across the Tibetan Plateau, Bull. Seism. Soc. Am., 65, 1051-1057, 1975.

Chun, K.Y., and T. Yoshii, Crustal structure of the Tibetan Plateau: A surface-wave study by a moving window analysis, Bull. Seism. Soc. Am., 67, 735-750, 1977.

Dziewonski, A.M., S. BLock, and M. Landisman, A technique for the analysis of transient seismic signals, Bull. Seism. Soc. Am., 59, 427-444, 1969.

Gupta, H.K., and H. Narain, Crustal structure in the Himalayan and Tibet Plateau, Bull. Seism. Soc. Am., 57, 235-248, 1967.

Mitchell, B.J., Regional Rayleigh wave attenuation in North America, J. Geophys. Res., 80, 4904-4916, 1975.

Molnar, P., T.J. Fitch, and F.T. Uki, Fault plane solutions of shallow earthquake and contemporary tectonics in Asia, Earth Planet. Sci. Lett., 19, 101-112, 1973.

Molnar, P., and P. Tapponmier, Cenozoic tectonics of Asia: Effects of a sontinental collision, Science, 189, 419-458, 1975.

Powell, C. McA., and P.J. Conaghan, Plate tectonics and the Himalayas, Earth Planet. Sci. Lett., 20, 1-12, 1973.

Santo, T., Lateral variation of Rayleigh wave dispersion character, Part II: Eurasia, Pure Appl. Geophys., 62, 67-80, 1965.

Yacoub, N.K., and B.J. Mitchell, Attenuation of Rayleigh-wave amplitudes across Eurasia, Bull. Seism. Soc. Am., 67, 751-769, 1977.

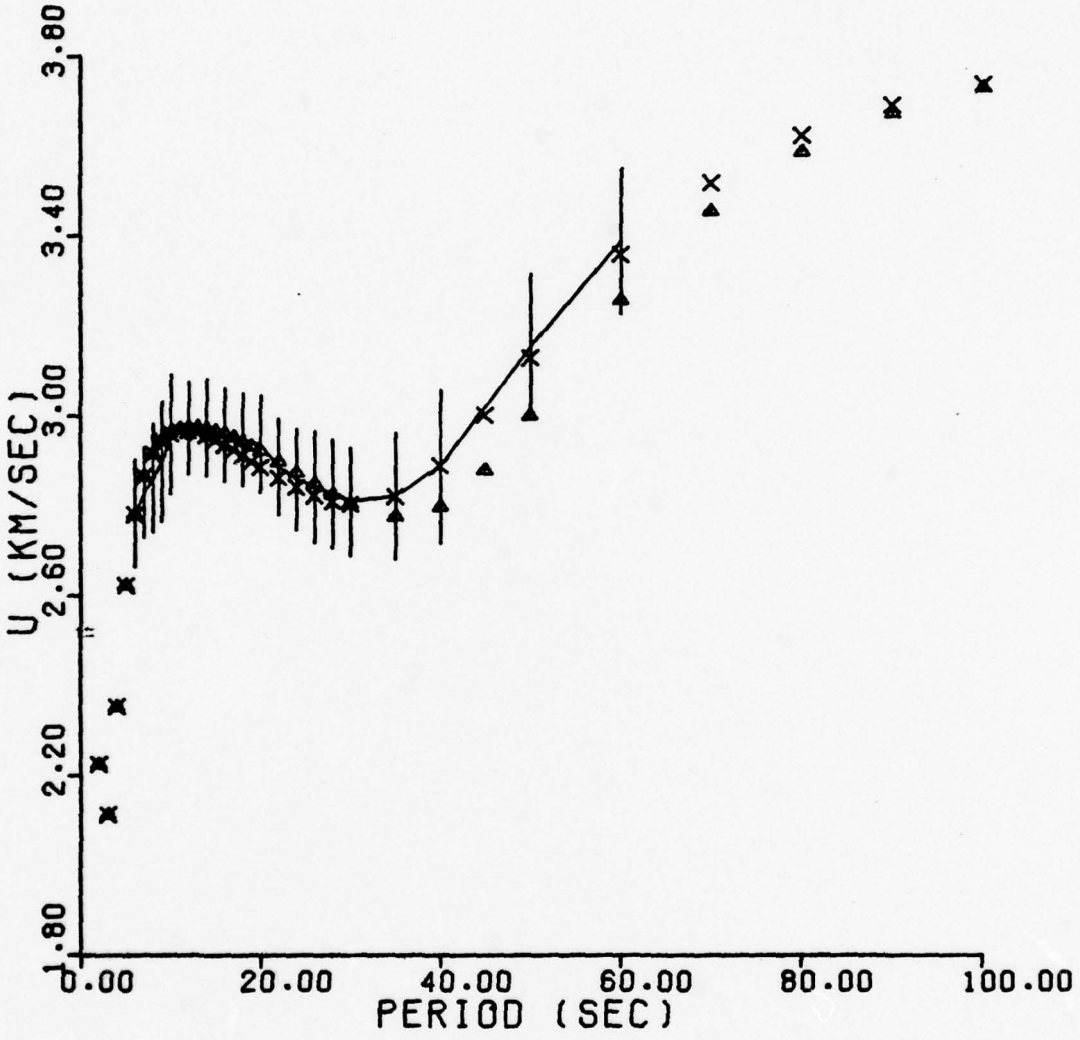

Figure 1. Dispersion curves for Tibetan Plateau. Crosses represent velocities for model A. Triangles represent group velocities for model TP-4. Solid line indicates the observed data from 30 paths across Tibetan Plateau with standard deviations marked by vertical lines.

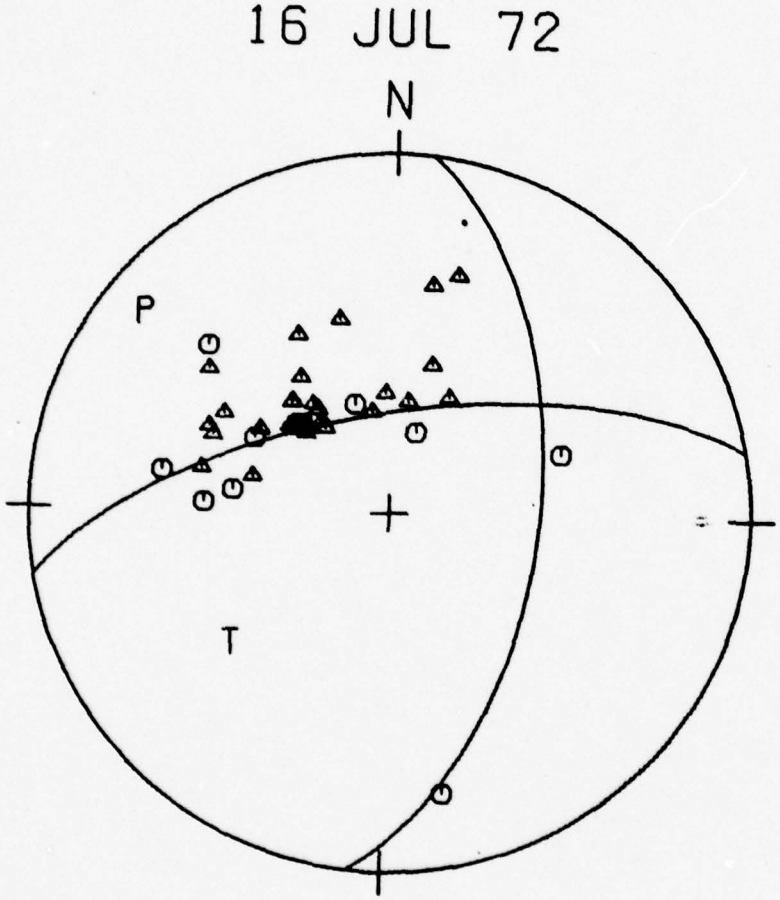

Figure 2. Fault plane solution. Compressions are indicated by octagons, dilatations by triangles.

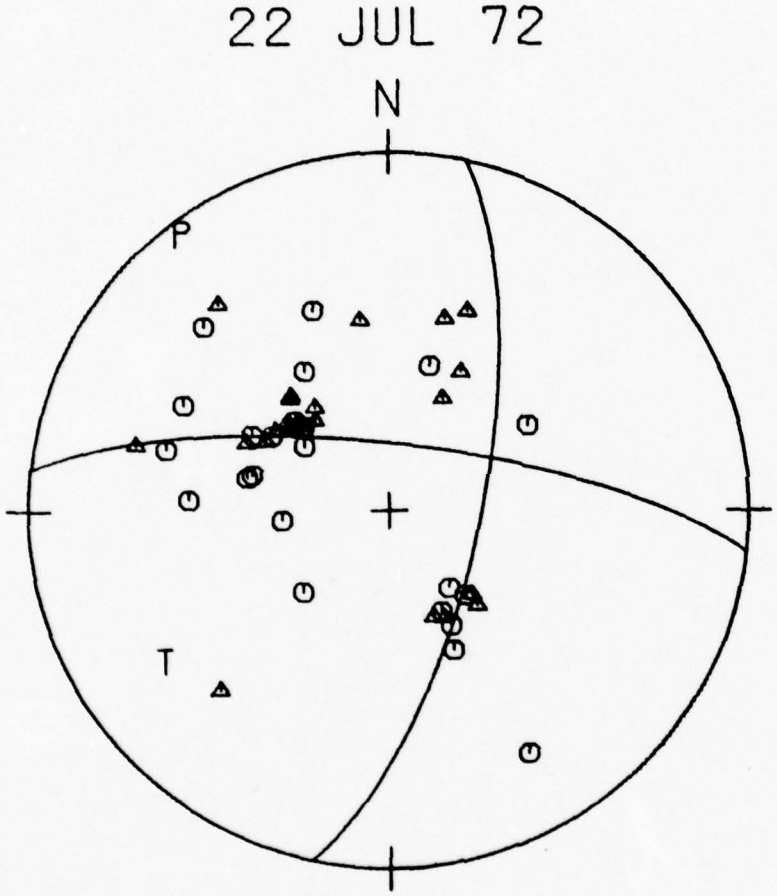

Figure 2a.

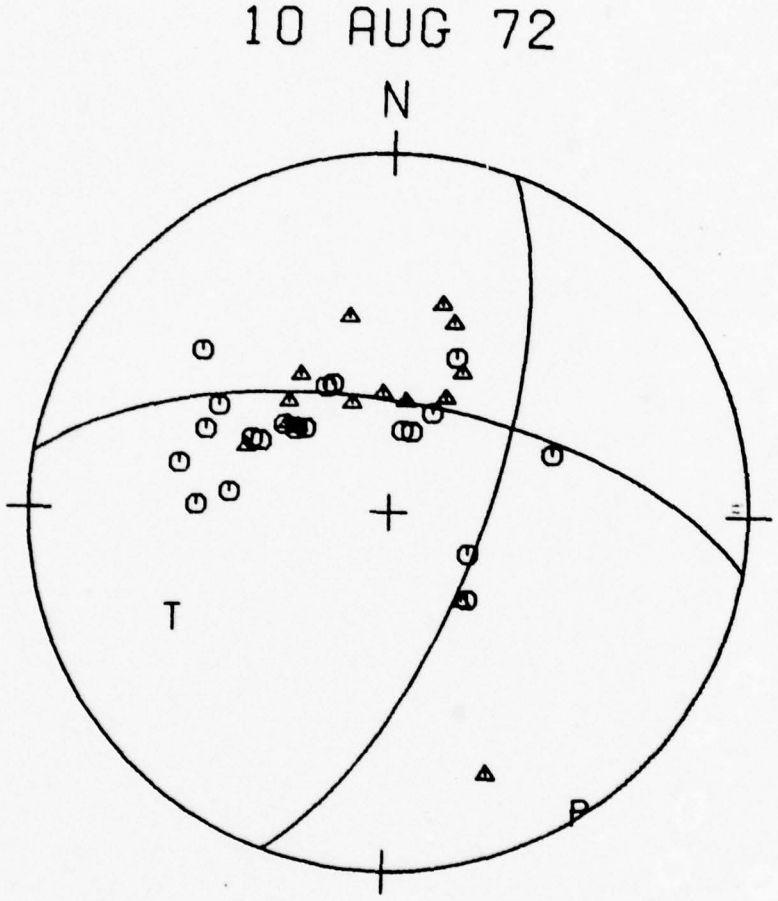

Figure 2b.

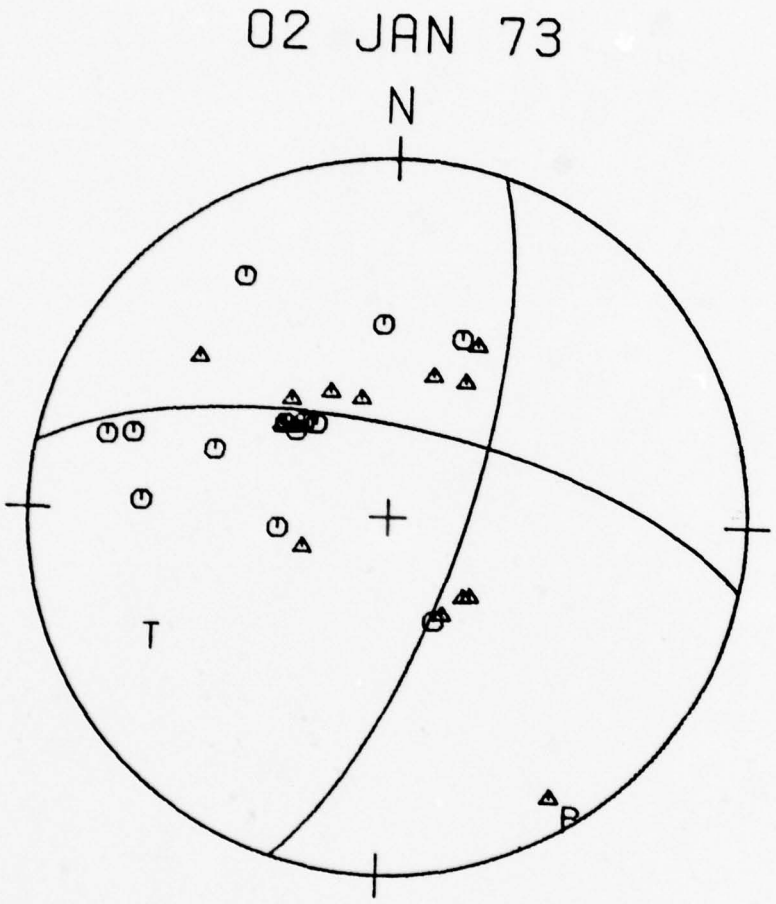

Figure 2c.

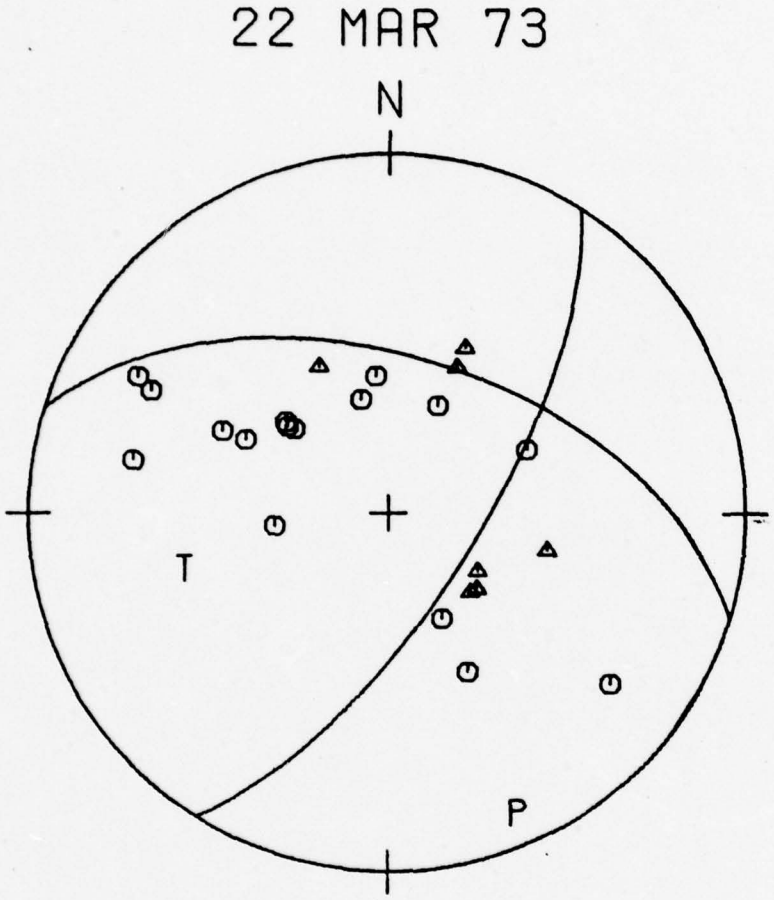

Figure 2d.

Table 1.

Earthquakes and stations used in the study

Date	Origin Time (UT)	Lat (^{o}N) (NEIC)	Long (^{o}E) (NEIC)	Depth (km)	m_b	M_s	Stations used for obtaining dispersion curve
1. 4 February 1972	14-08-21.7	30.4	84.6	18-N 18-I	5.2-N 5.1-I 5.01-W	4.9-M 3.92-W	NIL, SHL
2. 20 February 1972	03-02-14.6	34.6	80.3	33-N 33-I	4.8-N 4.8-I 4.79-W	4.7-M 3.51-W	SHL
3. 15 March 1972	06-00-32.4	30.4	84.5	33-N 12-N	5.3-N 5.1-I 5.07-W	4.7-M 4.07-W	NIL
4. 28 April 1972	00-52-56.8	31.3	84.9	33-N 32-I	5.1-N 5.0-I 5.16-W	4.5-M 4.26-W	NIL
5. 8 June 1972	23-10-12.0	29.5	92.3	64-N 73-I	4.7-N 4.6-I 4.8-M		NIL
6. 16 July 1972	02-20-23.6	32.5	95.9	33-N 19-I	5.2-N 5.1-I 5.3-M	4.8-M	NIL,KBL
7. 16 July 1972	03-39-59.8	32.6	95.8	33-N 37-I	4.7-N 4.6-I 5.0-M	5.0-M	NIL
8. 22 July 1972	16-41-4.0	31.4	91.5	33-N 17-I	5.5-N 5.4-I	5.8-N 5.8-M	NIL

9. 22 July 1972	21-00-08.6	31.4	91.4	33-N 33-I	4.7-N 4.6-I		NIL
10. 28 July 1972	15-31-42.6	31.4	91.4	33-N 8-N	4.3-N		NIL
11. 10 August 1972	21-06-40.1	32.4	93.5	33-N 34-I	5.2-N 5.0-I	4.8-N 4.6-M	KBL, NIL
12. 2 January 1973	22-25-57.0	31.2	88.1	33-N 43-I	5.2-N 5.1-I 5.2-M		NIL, KBL, SHL
13. 22 March 1973	01-06-57.2	28.1	87.0	33-N 33-I	5.2-N 5.0-I	5.0-M	NIL, KBL
14. 4 April 1973	17-53-08.2	30.5	83.7	48-N 48-I	4.8-N 4.5-I 4.4-M		SHL
15. 21 July 1973	19-50-06.3	35.1	86.4	33-N 9-I	5.3-N 4.9-I	4.9-M	SHL
16. 1 August 1973	14-05-16.2	29.6	89.1	71-N 63-I	4.9-N 4.9-I 5.0-M	4.5-M	NIL
17. 21 November 1973	19-47-56.3	34.7	81.0	26-N 25-I	5.0-N 5.1-I	5.2-N 4.9-M	SHL
18. 26 November 1973	21-53-33.0	34.4	91.6	33-N 15-I	4.6-N 4.3-I		NIL, SHL
19. 27 November 1973	09-31-10.8	33.0	86.7	33-N 33-I	5.0-N 4.9-I 5.1-M	4.7-M	NIL, SHL
20. 3 March 1974	04-53-15.6	30.8	86.3	33-N 29-I	5.3-N 5.4-I	5.5-M	NIL

21. 6 March 1974	17-36-21.2	32.3	85.7	33-N 29-I	4.7-N 4.5-I	SHL
22. 2 July 1974	16-25-53.3	35.6	80.9	33-N 33-I	4.7-N 4.6-I 5.0-M	SHL

* N - values were determined by NEIC
  I - values were determined by ISC
  M - values were determined by Moscow
  W - values were determined by us

Table 2.

Group velocities of fundamental-mode Rayleigh waves

period (Sec)	observed averaged value (km/sec)	observed standard deviation (km/sec)	model A	model TP-4
2			2.224	2.224
3			2.112	2.112
4			2.352	2.352
5			2.622	2.622
6	2.784	0.120	2.779	2.780
7	2.829	0.100	2.865	2.866
8	2.862	0.121	2.915	2.915
9	2.899	0.134	2.943	2.945
10	2.960	0.133	2.959	2.962
12	2.974	0.103	2.967	2.976
14	2.975	0.108	2.956	2.973
16	2.959	0.104	2.936	2.962
18	2.949	0.103	2.912	2.944
20	2.938	0.108	2.886	2.922
22	2.888	0.107	2.862	2.898
24	2.860	0.113	2.841	2.874
26	2.842	0.125	2.822	2.849
28	2.827	0.121	2.809	2.825
30	2.809	0.120	2.803	2.804
35	2.821	0.141	2.820	2.775

40	2.888	0.171	2.890	2.798
50	3.155	0.162	3.129	3.000
60	3.388	0.162	3.359	3.257
70			3.518	3.455
80			3.623	3.586
90			3.691	3.672
100			3.737	3.730

Table 3.

Tibetan velocity model

model	thickness (km)	P velocity (km/sec)	S velocity (km/sec)	density (g/cm^3)
TP-4	3.50	4.50	2.60	2.40
	8.50	5.98	3.45	2.80
	16.00	5.98	3.42	2.80
	10.00	5.80	3.37	2.75
	30.00	6.30	3.64	2.90
		7.70	4.45	3.30
A	3.50	4.50	2.60	2.40
	8.50	5.98	3.45	2.80
	16.00	5.98	3.42	2.80
	10.00	5.80	3.37	2.75
	30.00	6.60	3.81	2.90
		7.70	4.45	3.30

Frequency Dependence of Q_β in the Continental Crust

by

Brian J. Mitchell

Introduction

Inversions of surface wave attenuation data to obtain internal friction (Q_β^{-1}) models of the crust and upper mantle usually assume that the degree of frequency dependence of Q_β is small enough to be ignored. Most Q_β^{-1} models of the continental crust and upper mantle (e.g. Mitchell, 1973b; Lee and Solomon, 1975; Herrmann and Mitchell, 1975; Mitchell, 1975) are consequently dependent upon the assumption that Q_β is independent of frequency. The purpose of this report will be to combine higher and fundamental modes to test the appropriateness of the frequency-independence assumption in the inversion of seismic surface wave attenuation data.

The phase Lg is often the largest phase on short-period seismograms recorded at regional distances. In the frequency band 10 Hz to about 2 seconds, Lg consists of a superposition of numerous higher-mode Rayleigh waves (Knopoff et al., 1973). At longer periods (about 4-10 s), it is often possible to isolate one or two higher modes. If the nature of the frequency dependence of Q_β can be established, then it should be possible to predict the attenuation of high-frequency (1 Hz) Lg waves from longer-period higher-mode data, and vice versa.

Data

The most extensive set of surface wave attenuation data at intermediate periods in continental regions has been obtained in eastern North America (Herrmann and Mitchell, 1975). The only higher mode attenuation data in the period range 4-10 seconds have also been obtained for that region (Mitchell, 1973a; Herrmann, 1973). Fundamental-mode attenuation data in the period range 4-40 s will be combined with data at a period of 0.4 s (Kurz and Redpath, 1968) to obtain new Q_β^{-1} models of the crust in eastern North America. The models which are obtained are then used to calculate higher-mode attenuation coefficients for comparison with the observed attenuation coefficients of the higher modes between 4 and 10 s and with the observed attenuation coefficients for Lg at shorter periods in eastern North America (Nuttli, 1973; Street, 1976; Bollinger, 1979; Pomeroy, 1977; Nuttli and Dwyer, 1978). The details of the method are described below.

Procedure and Results

The amplitude of particle motion of the higher Rayleigh modes, even at relatively short periods, is significant to large depths in the crust (Figure 1). Amplitudes of the higher modes, for this reason, can be compared to those of the fundamental mode to investigate the frequency dependence of shear wave internal friction (Q_β^{-1}) in the crust.

The first step in the process of investigating the frequency dependence of Q_β in the crust is to obtain models of Q_β^{-1} as a function of depth from fundamental-mode Rayleigh-wave attenuation data. In

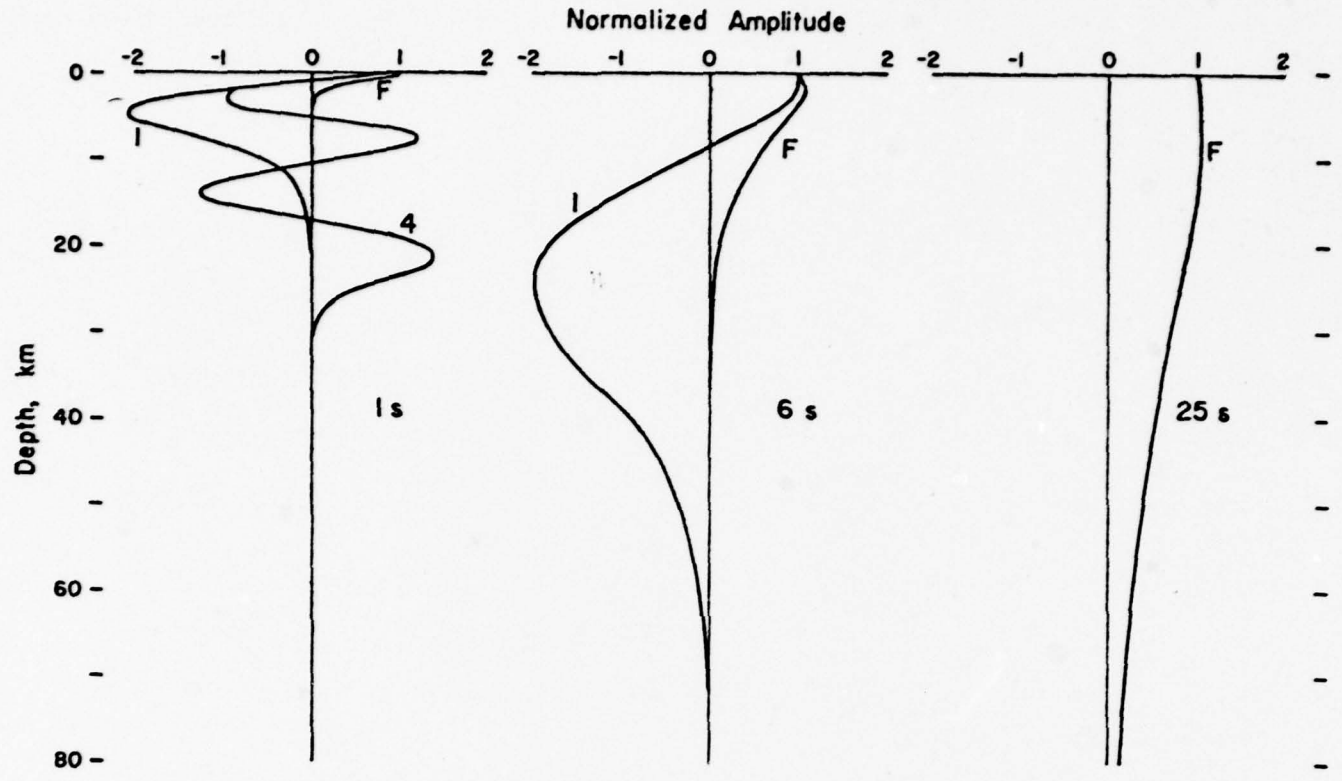

Figure 1. Normalized amplitudes of particle motion for 3 periods predicted by the eastern United States model of Mitchell and Herrmann (1979). The letter F denotes the fundamental mode and the number by each curve denotes the number of the higher mode.

obtaining those models I assume that Q_β is frequency dependent such that $Q_\beta(\omega,z) = C(z)\omega^\alpha$ where ω is angular frequency and α is a constant. The case $\alpha = 0$ corresponds to the case where Q_β is independent of frequency. It is possible to satisfy the fundamental mode data with a wide range of values for α. Two cases ($\alpha = 0.0$ and 0.5) appear in Figure 2.

The next step is to do the forward problem of calculating attenuation coefficients for the higher modes using the models obtained from inversion of the fundamental-mode data. A difficulty in this process is that the observed higher-mode data sometimes correspond to a single mode and sometimes to several modes. This problem is illustrated by Figures 3 and 4 where theoretical group velocities for the eastern United States model of Mitchell and Herrmann (1979) and theoretical spectral amplitudes for that model and selected event-station examples are plotted. It is apparent that higher-mode observations at velocities of about 3.5 km/sec in the eastern United States consist predominantly of the first higher mode at periods greater than about 3 seconds. At shorter periods there is much overlap in group velocities for the various modes and several modes contribute to the observed Lg wave form. However, Lg attenuation coefficients are usually determined for waves travelling at group velocities between 3.3 and 3.6 km/sec. If that is the case, an average attenuation coefficient for the first four higher modes should approximate the attenuation coefficient for Lg at a period of 1 second. At a period of 2 seconds, the first two higher modes should be sufficient.

Figure 5 presents observed higher-mode attenuation coefficients and theoretical coefficients for various values of α, assuming that

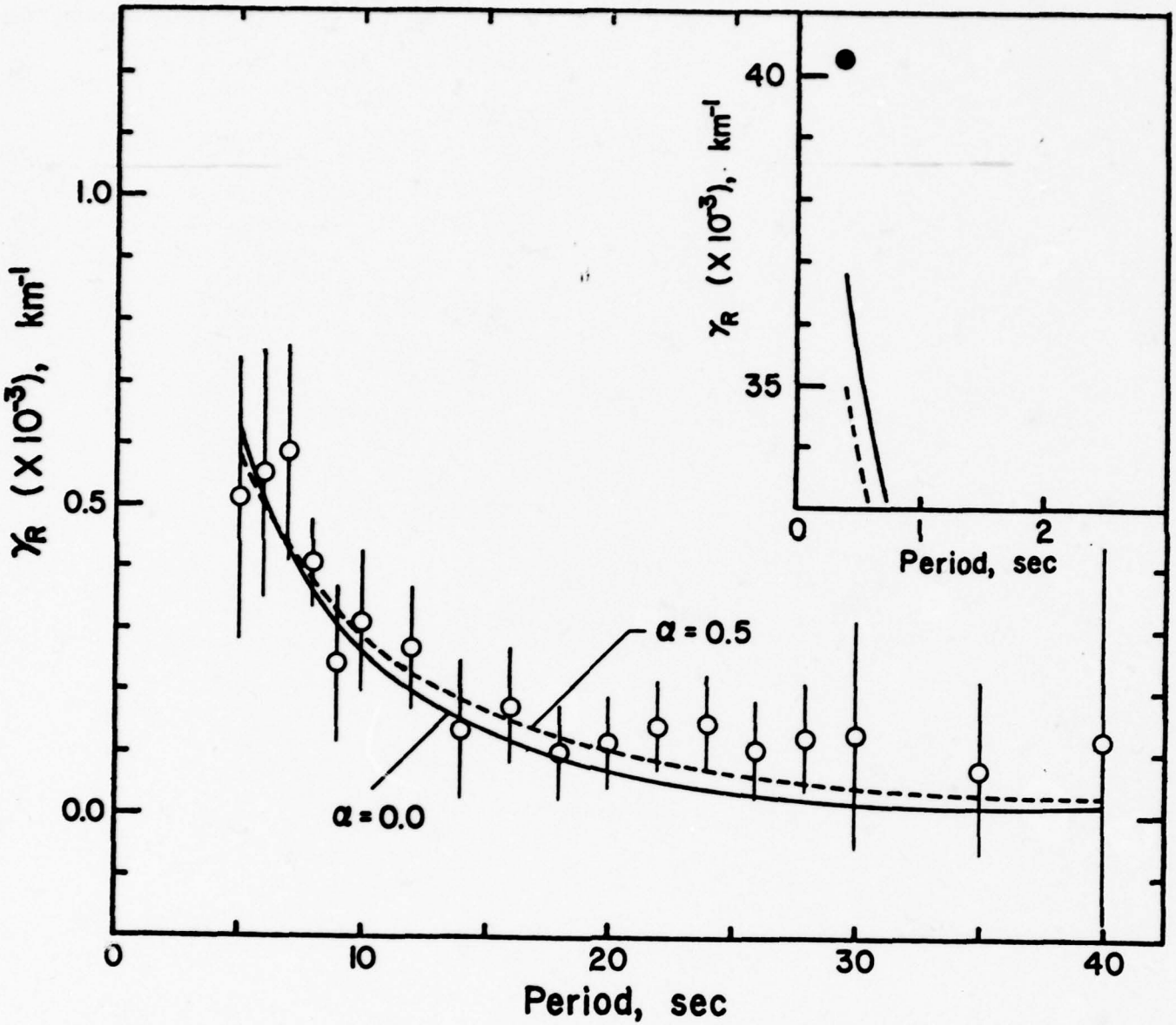

Figure 2. Observed attenuation coefficients for the fundamental Rayleigh mode. Open circles and vertical lines are the values and standard deviations observed by Herrmann and Mitchell (1975). The closed circle is a data point from Kurz and Redpath (1968).

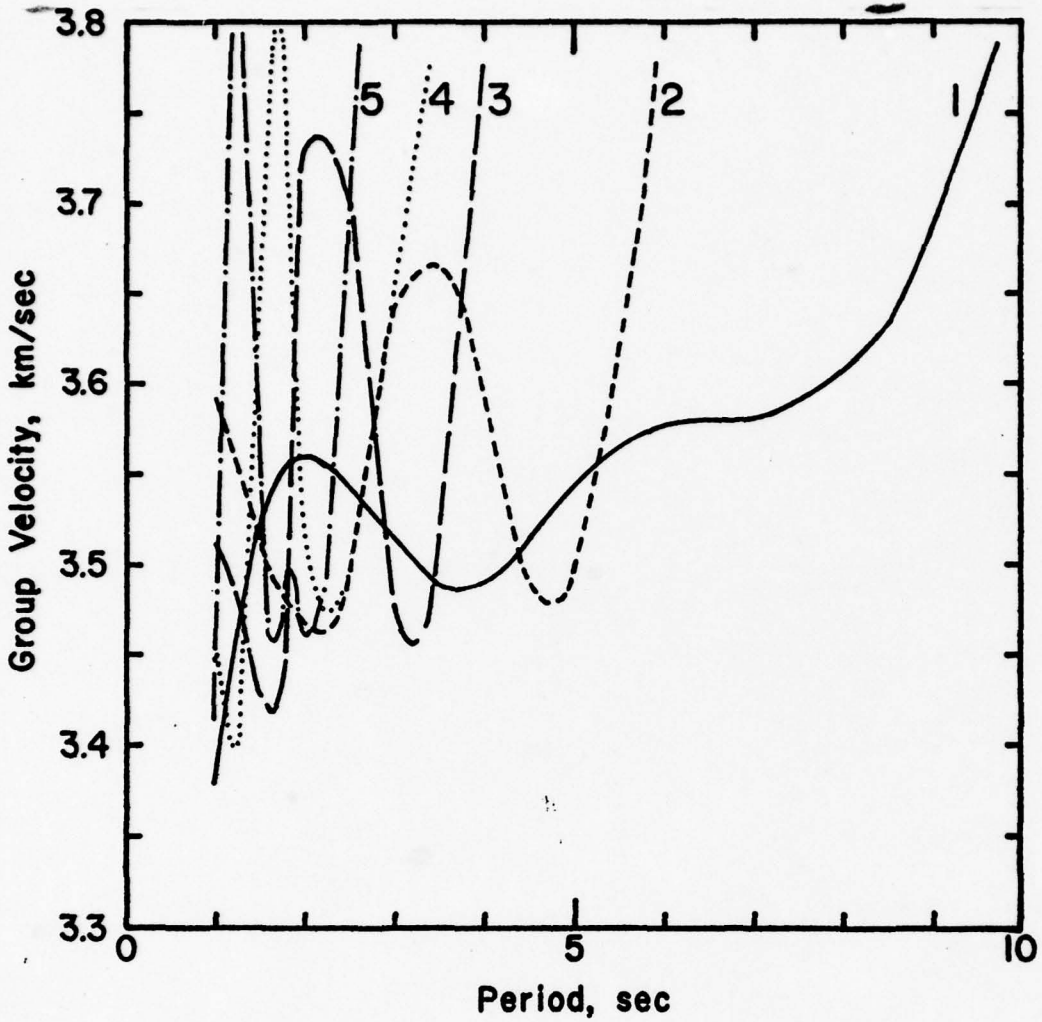

Figure 3. Theoretical group velocities of the first 5 higher Rayleigh modes for the eastern United States model of Mitchell and Herrmann (1979).

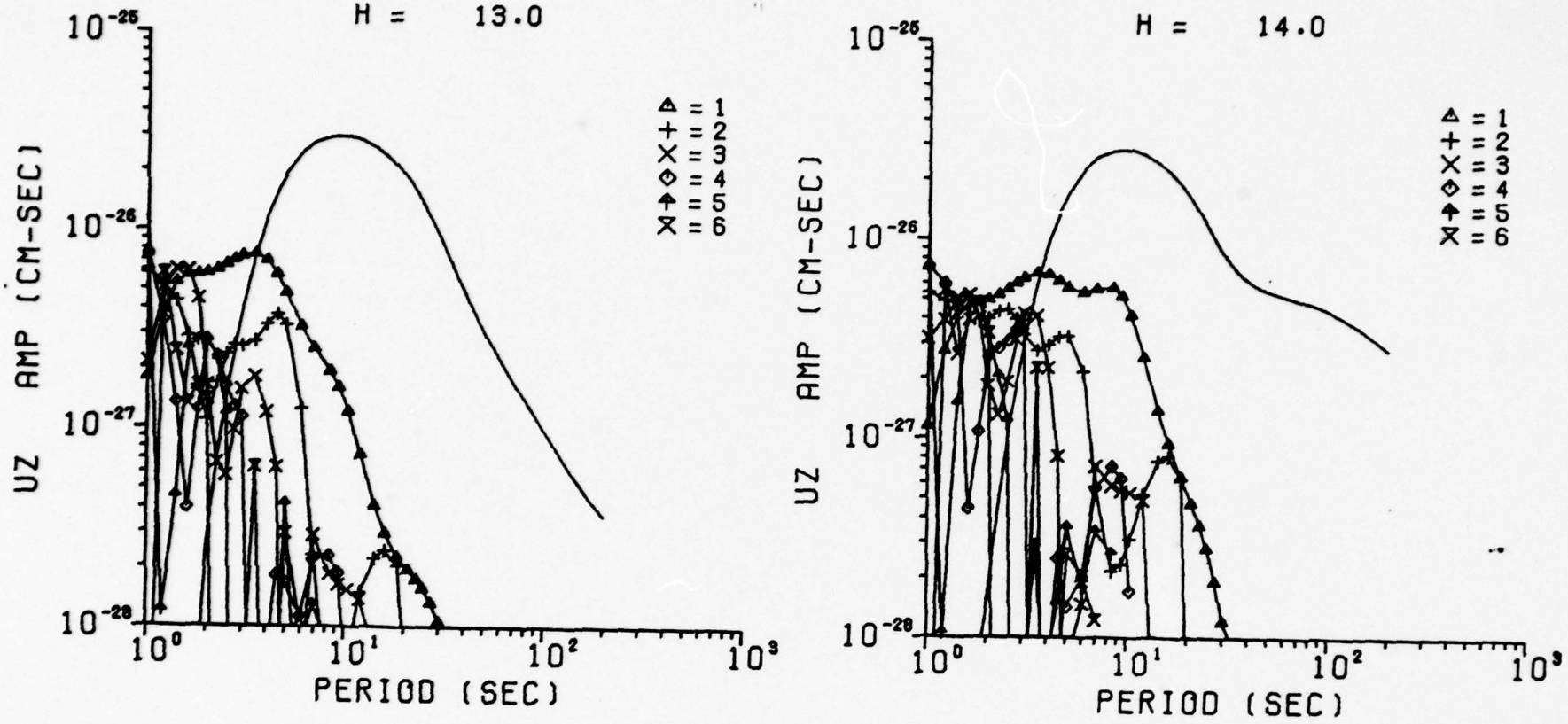

Figure 4. Theoretical amplitude spectra of the fundamental and 6 higher Rayleigh modes for the eastern United States model of Mitchell and Herrmann (1979). (Left) The earthquake of 3 March 1963 as recorded at station AAM. (Right) The earthquake of 17 November 1970 as recorded at station ATL.

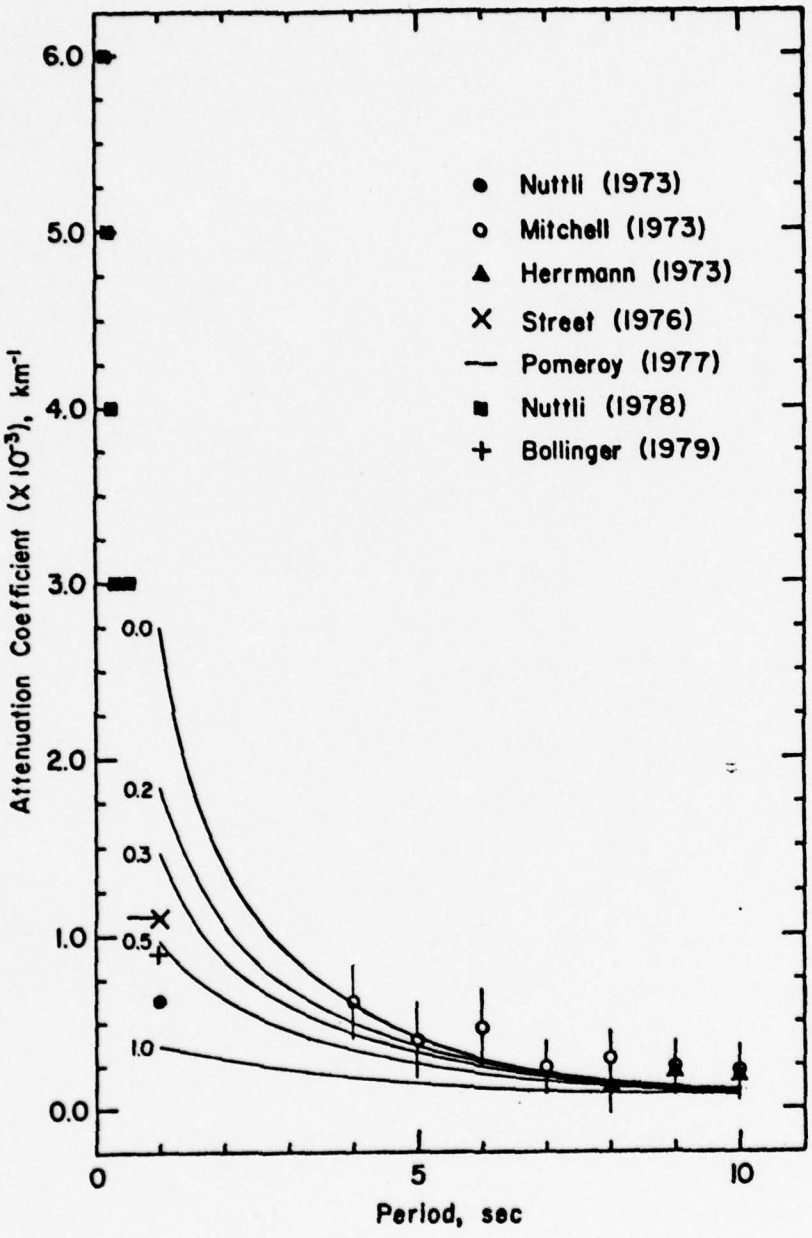

Figure 5. Fit of theoretical higher-mode attenuation coefficients to observed values for various values of α, assuming that α is constant over the entire period range 1-40 seconds.

α is a constant throughout the entire period range between 1 and 40 seconds. It is clear that a frequency independent (α = 0.0) Q_β^{-1} model will not satisfy the higher-mode attenuation data. Further, it appears that none of the models for which α is a constant throughout the entire period range fit the data very well. The case α = 0.3, perhaps, comes closest to explaining all of the data.

Additional models were explored in which α was allowed to vary with frequency. Attenuation coefficients for some of these models appear in Figures 6 and 7. A very good fit to the data was achieved for the case in which α was set equal to zero at periods greater than 4 seconds and equal to 0.5 at periods of 4 seconds or less. The hump in the curve corresponds to the jump in α at a period of 4 seconds and can be smoothed out with a less abrupt change in α. Good fits to the data can also be achieved by letting α increase gradually with decreasing period at periods less than 4 seconds. Two such cases appear in Figure 7 where α is set at values of 0.0 and 0.2 at long periods. Undoubtedly, several other distributions of α over the period range 1-40 seconds will also satisfy the higher-mode attenuation data.

There are several Q_β^{-1} models for the crust of eastern North America which might explain the fundamental and higher-mode data. A frequency-independent model and a model for the case of constant α (= 0.3) over the entire frequency range between 1 and 40 seconds appear in Figure 8. Some models for which α varies with period are presented in Figure 9. Comparisons of the theoretical attenuation coefficient values to the observations (Figures 5-7) indicate that the cases for which α increases with decreasing period are better than those for which α is a constant.

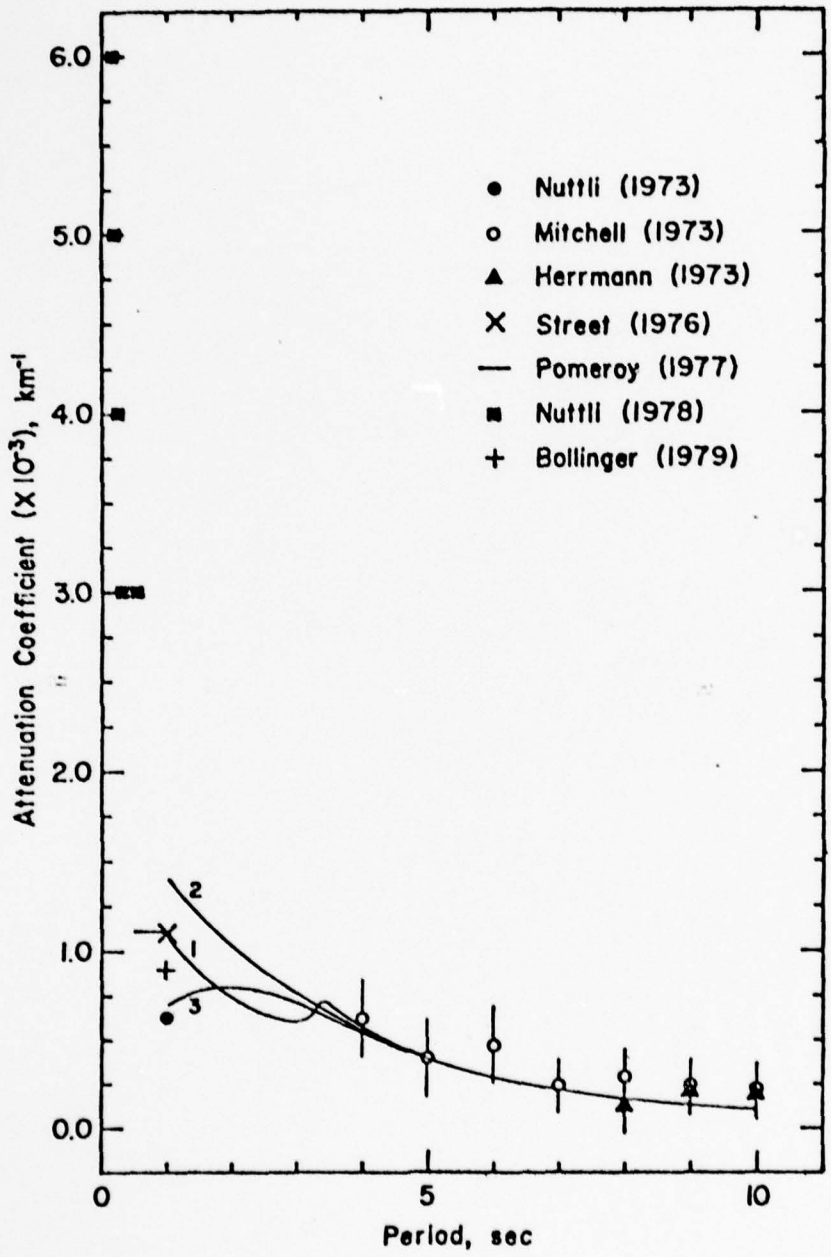

Figure 6. Fit of theoretical higher-mode attenuation coefficients to observed values for various values of α. (1) $\alpha = 0.0$ for $T > 4$ seconds, $\alpha = 0.5$ for $1 < T < 4$ seconds. (2) $\alpha = 0.0$ for $T > 4$ seconds, $0.72 < \alpha < 0.0$ for $1 < T < 4$ seconds. (3) $\alpha = 0.0$ for $T > 4$ seconds, $0.4 < \alpha < 0.0$ for $1 < T < 4$ seconds.

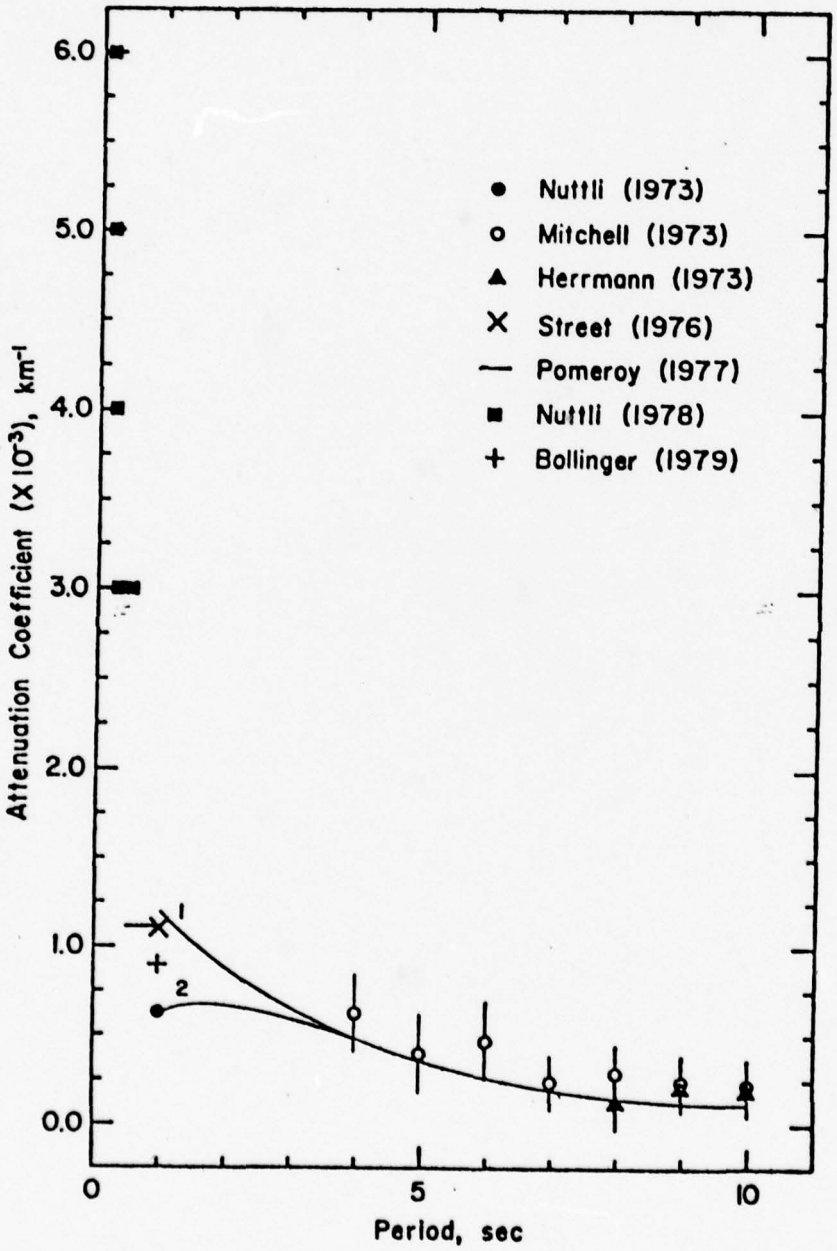

Figure 7. Fit of theoretical higher-mode attenuation coefficients to observed values for various values of α. (1) $\alpha = 0.2$ for $T > 5$ seconds, $0.4 > \alpha > 0.2$ for $1 < T < 5$ seconds. (2) $\alpha = 0.2$ for $T > 5$ seconds, $0.75 > \alpha > 0.2$ for $1 < T < 5$ seconds.

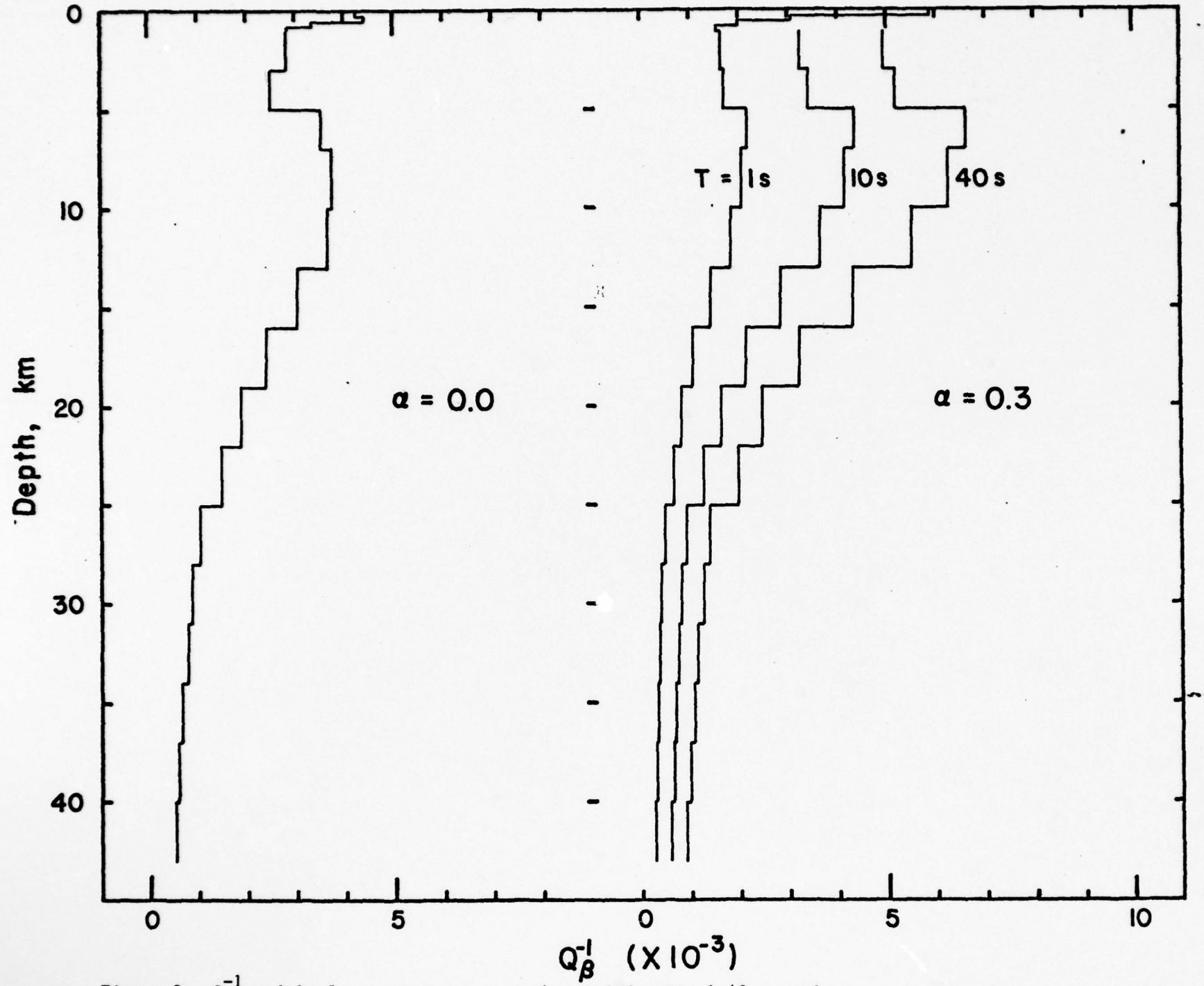

Figure 8. Q_β^{-1} models for α constant over the period range 1-40 seconds.

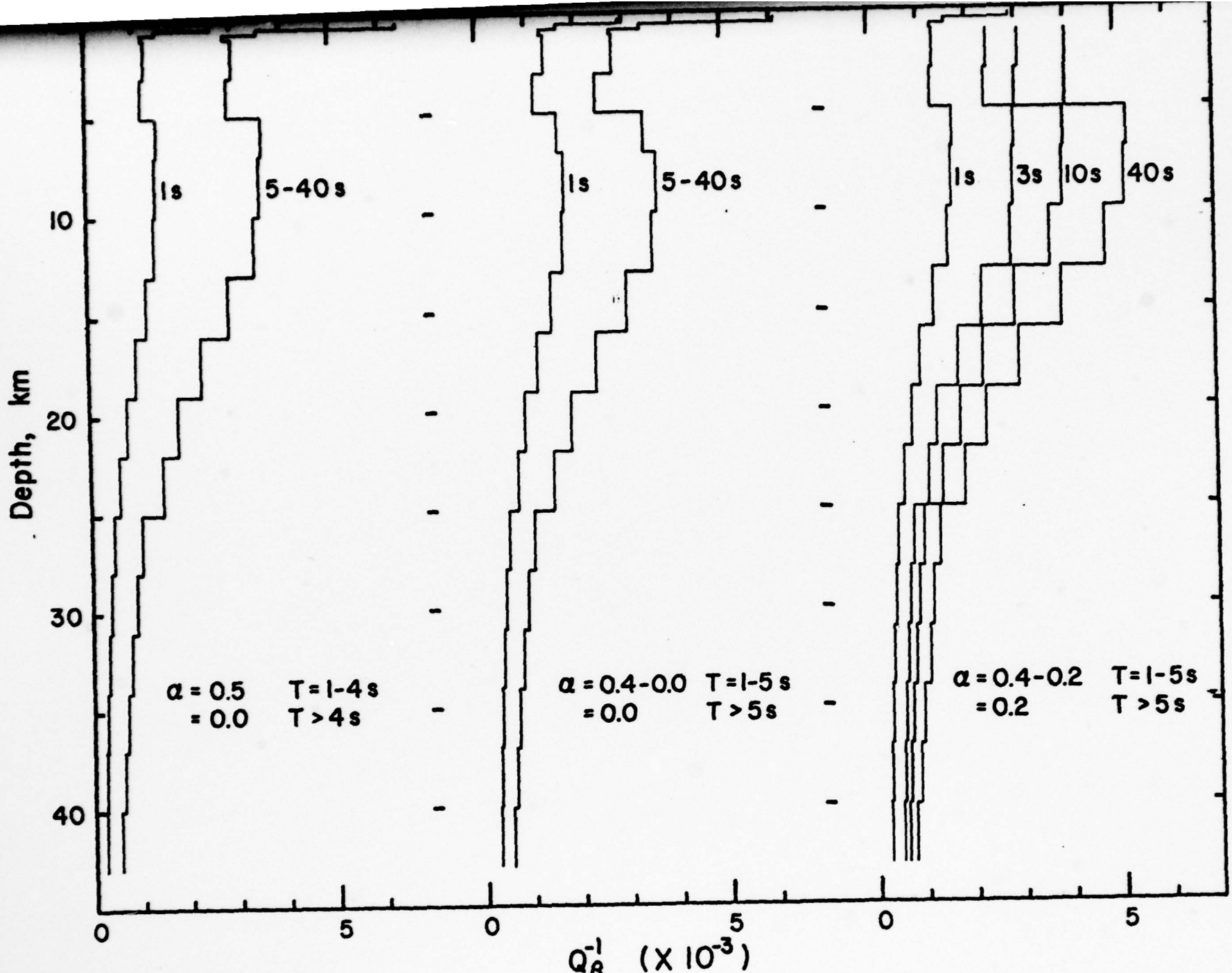

Figure 9. Q_β^{-1} models for α variable over the period range 1-40 seconds.

References

Bollinger, G.A., Attenuation of the Lg phase and the determination of m_b in the Southeastern United States, Bull. Seism. Soc. Am., 69, 45-63, 1979.

Herrmann, R.B., Surface wave generation by the south central Illinois earthquake of November 9, 1968, Bull. Seism. Soc. Am., 63, 2121-2134, 1973.

Herrmann, R.B., and B.J. Mitchell, Statistical analysis and interpretation of surface wave anelastic attenuation data for the stable interior of North America, Bull. Seism. Soc. Am., 65, 1115-1128, 1975.

Knopoff, L., F. Schwab, and E. Kausel, Interpretation of Lg, Geophys. J. Roy. Ast. Soc., 33, 389-404, 1973.

Kurz, M.K., Jr., and B.B. Redpath, Project Pre-Gondola, Seismic Site Calibration, Report PNE-1100, May 1968, U.S. Army Nuclear Cratering Group, CE, Livermore, Cal., 1968.

Lee, W.B., and S.C. Solomon, Inversion schemes for surface wave attenuation and Q in the crust and mantle, Geophys. J. Roy. Ast. Soc., 43, 47-71, 1975.

Mitchell, B.J., Radiation and attenuation of Rayleigh waves from the southeastern Missouri earthquake of October 21, 1965, J. Geophys. Res., 78, 886-899, 1973a.

Mitchell, B.J., Surface wave attenuation and crustal anelasticity in central North America, Bull. Seism. Soc. Am., 63, 1057-1071, 1973b.

Mitchell, B.J., Regional Rayleigh wave attenuation in North America, J. Geophys. Res., 4904-4916, 1975.

Mitchell, B.J., and R.B. Herrmann, Shear velocity structure in the eastern United States from the inversion of surface wave group and phase velocities, Bull. Seism. Soc. Am., in press, 1979.

Nuttli, O.W., Seismic wave attenuation and magnitude relations for eastern North America, J. Geophys. Res., 78, 876-885, 1973.

Nuttli, O.W., and J.J. Dwyer, Attenuation of high-frequency seismic waves in the central Mississippi Valley, Waterways Exp. Sta., Corps of Eng., Vicksburg, Miss., July, 1978.

Pomeroy, P.W., Aspects of Seismic Wave Propagation in Eastern North America, A Preliminary Report, Roundout Associates, 1977.

Street, R.L., Scaling northeastern United States/southeastern Canada earthquakes by their Lg waves, Bull. Seism. Soc. Am., 66, 1525-1537, 1976.

Higher-Mode Attenuation in the Middle East---
Iran to Turkey

by

Brian J. Mitchell

Introduction

Methods previously developed to determine shear wave internal friction models in North America are being used to study the attenuation of higher-mode Rayleigh waves in the Middle East. Although this work is still in progress, preliminary results have been obtained which are important to understanding surface wave propagation and attenuation through a portion of the Middle East from eastern Iran to western Turkey.

Data

As described in other sections of this report, higher modes with periods of a few seconds will be combined with fundamental-mode data to study the anelastic properties of the earth's crust. The method requires the use of sources for which the depths and fault-plane solutions are known. Fault-plane solutions for several suitably located earthquakes in the Middle East have been determined by McKenzie (1972). They are listed in Table 1 and appear on a map in Figure 1. The paths cover an east-west trending region from eastern Iran to western Turkey, most of which is comprised of plateaus and small mountain ranges.

The essential data consist of Rayleigh wave amplitude data, both fundamental and higher modes. In addition to the amplitude data,

Table 1.

Description of Earthquake Sources

No.	Date	Origin Time	Latitude (N)	Longitude (E)	Depth (km)	Magnitude	Azimuth	Dip	Azimuth	Dip
1	27 Apr 66	19 48 52.4	38.20	42.50	40	5.0	15°	67°	112°	74°
2	27 Jul 66	14 49 02.1	32.60	48.80	33	5.3	80°	59°	114°	34°
3	7 Apr 67	18 33 31.3	37.40	36.20	39	5.0	~45°	~90°	~135°	~90°
4	29 Apr 68	17 01 57.6	39.20	44.30	34	5.3	59°	70°	140°	66°
5	4 Sep 68	23 24 47.2	33.99	58.24	15	5.4	147°	65°	147°	25°

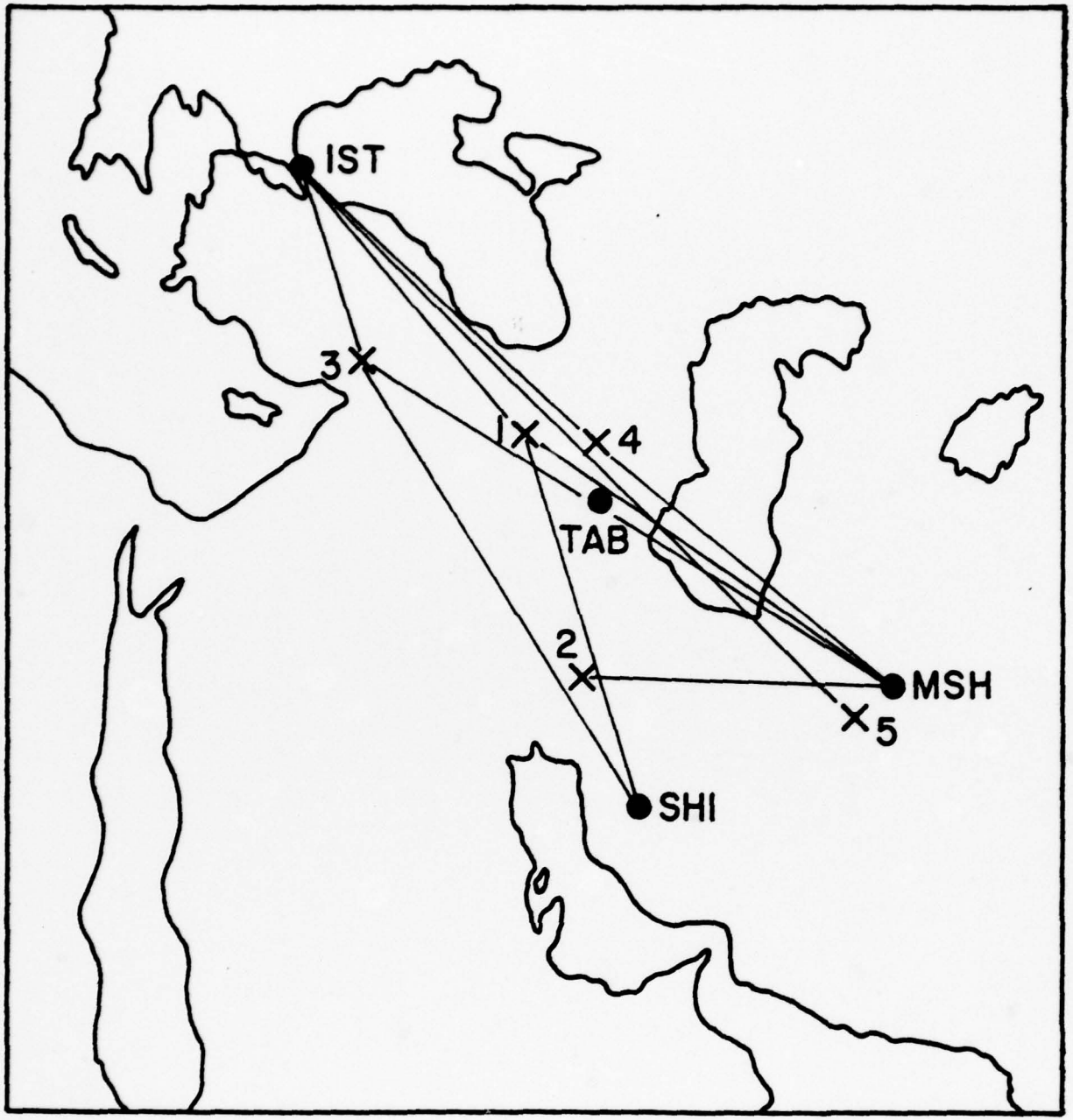

Figure 1. Map of the Middle East indicating the earthquakes and stations used in this study.

however, group velocity data are also required in order to establish a crustal model for that region. Both these types of data have been obtained using the multiple-filter method. The group velocities are plotted in Figure 2. It is interesting to note that the higher-mode velocities are observed only to periods as great as about 6 seconds. By comparison, higher modes are observed in eastern North America to periods as large as about 10 seconds. The scatter in both the fundamental- and higher-mode Rayleigh wave group velocity data is quite large, probably because of the complexity of the crust in that region. The group velocities are quite low, indicating that the shear velocities in the crust of that region of the Middle East are lower than those which would be expected for a shield or stable region.

Method and Preliminary Results

In order to apply our method to obtain attenuation data and Q models for the portion of the Middle East between eastern Iran and western Turkey, it is first necessary to obtain a model of seismic velocities and densities. Since, to our knowledge, no crustal model is available for that region, it is necessary to obtain a model by using the group velocity data of the present study. Because of the relatively large scatter in the observations, it was decided to obtain a model by simple trial-and-error fitting of the data. The solid lines in Figure 2 indicate the theoretical group velocities for the model in Table 2. It is interesting to note that the model is very similar to the model of Bucher and Smith (1971) for the Colorado Plateau in the western United States, differing only by having one layer which is 1½ km thicker than the corresponding layer in the Colorado Plateau.

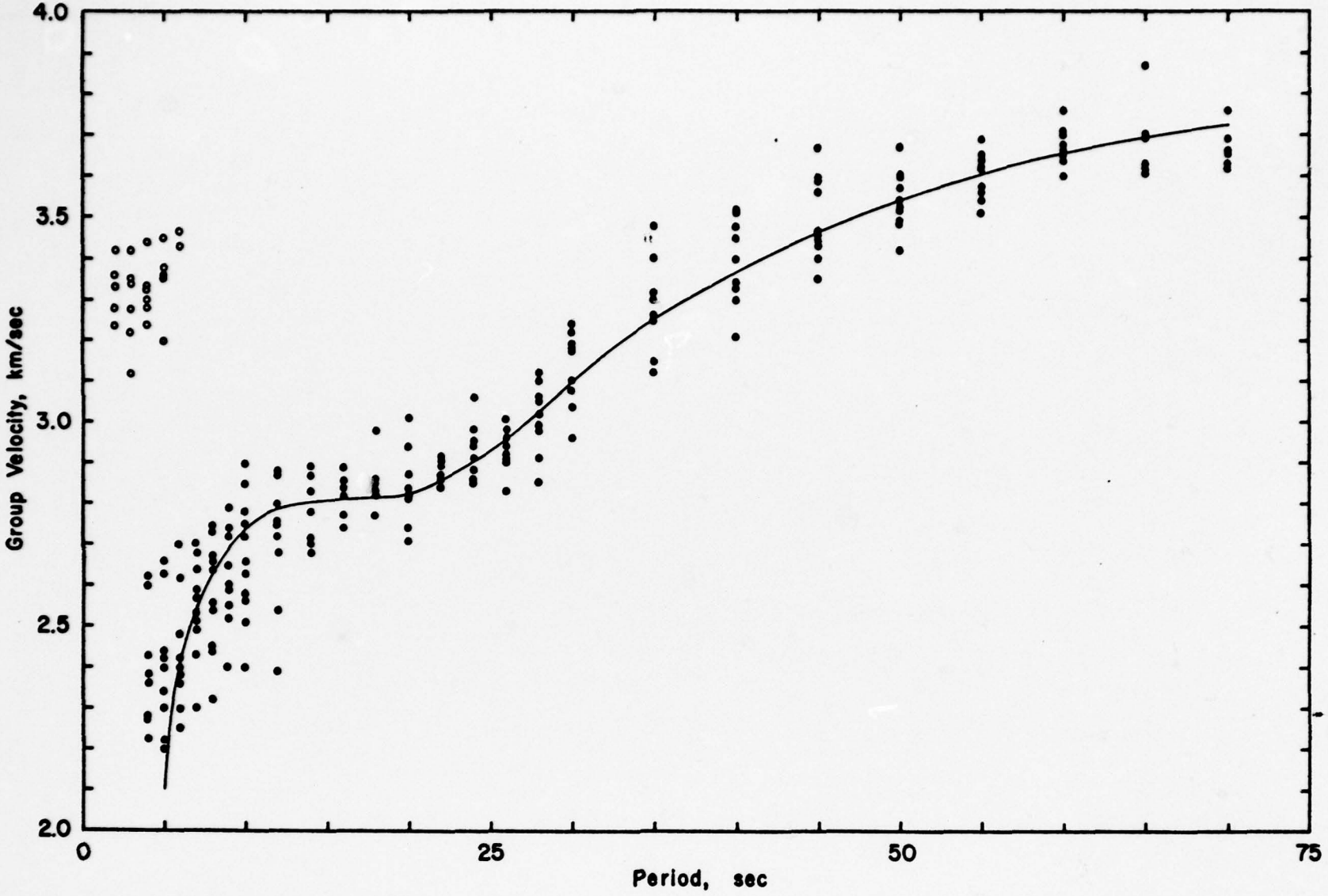

Figure 2. Observed fundamental-mode (closed circles) and higher-mode (open circles) Rayleigh wave group velocities across Iran and Turkey. The solid line indicates theoretical values for the crustal model in Table 2.

Table 2.

Crustal Model

Thickness (km)	P velocity (km/sec)	S velocity (km/sec)	Density (gm/cm^3)
2.5	3.0	1.73	2.40
26.0	6.2	3.58	2.83
13.0	6.8	3.87	2.99
45.0	7.8	4.25	3.30
----	8.2	4.38	3.43

The availability of a crustal model and sources with known depths and fault-plane solutions permits the calculation of surface wave amplitude spectra (Levshin and Yarson, 1971; programmed by R.B. Herrmann) for the fundamental and higher modes. Examples of these spectra appear in Figures 3 and 4, where they are compared with observed spectra for the earthquake of 27 July 1966 assuming two different focal depths. Figure 3 compares observed spectral amplitudes with theoretical values corresponding to a source depth of 40 km and Figure 4 compares the observed values to theoretical values for a source depth of 20 km. The greater depth is the value given by the USGS location. In both cases the observed higher mode spectral amplitudes are much smaller than those predicted by theory. This result indicates severe attenuation of higher modes, either by low Q values in the crust or by scattering produced by inhomogeneities. If the focal depth for the earthquake is 40 km, it is likely that scattering of the higher modes is most important, since the fundamental mode spectral amplitudes in Figure 3 exhibit little attenuation. If the focal depth is near 20 km, however, anelastic attenuation is likely to be the important mechanism. since both higher modes and the short-period fundamental mode spectral amplitudes in Figure 4 exhibit large attenuation. The position of the spectral minimum in the observations at a period of about 40 seconds corresponds more closely to the theoretical spectral hole for the case of the shallower source. This preliminary result indicates that low Q is likely to characterize the crust of Iran and Turkey. Further studies should provide enough data to yield a Q model for that region which will explain both fundamental-mode and

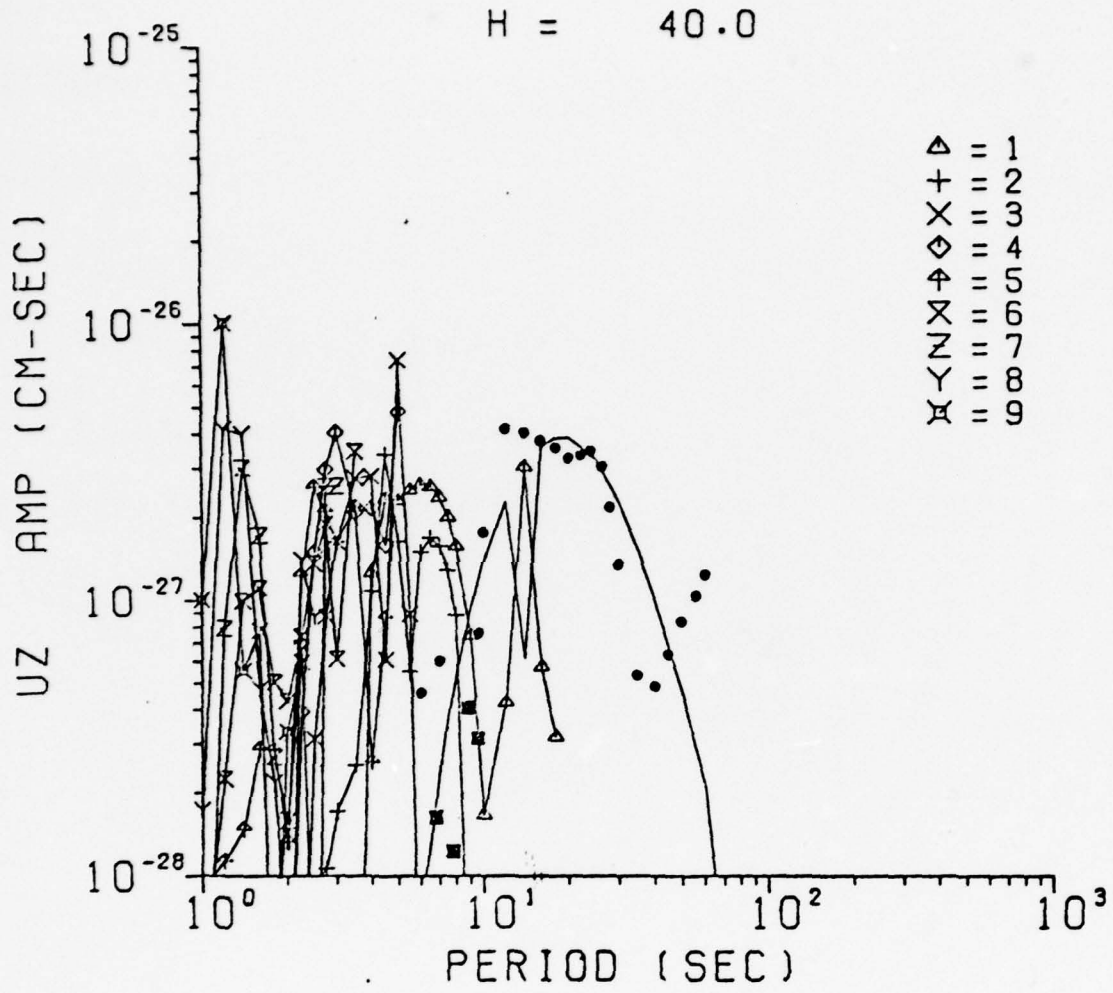

Figure 3. Amplitude spectra of Rayleigh waves for the earthquake of 27 July 1966 as recorded at station MSH. Closed circles denote observed fundamental-mode values and open circles denote observed higher-mode values. Theoretical values for the fundamental-mode are indicated by the solid line and for the higher-modes by the symbols on the right side of the figure. The assumed focal depth is 40 km.

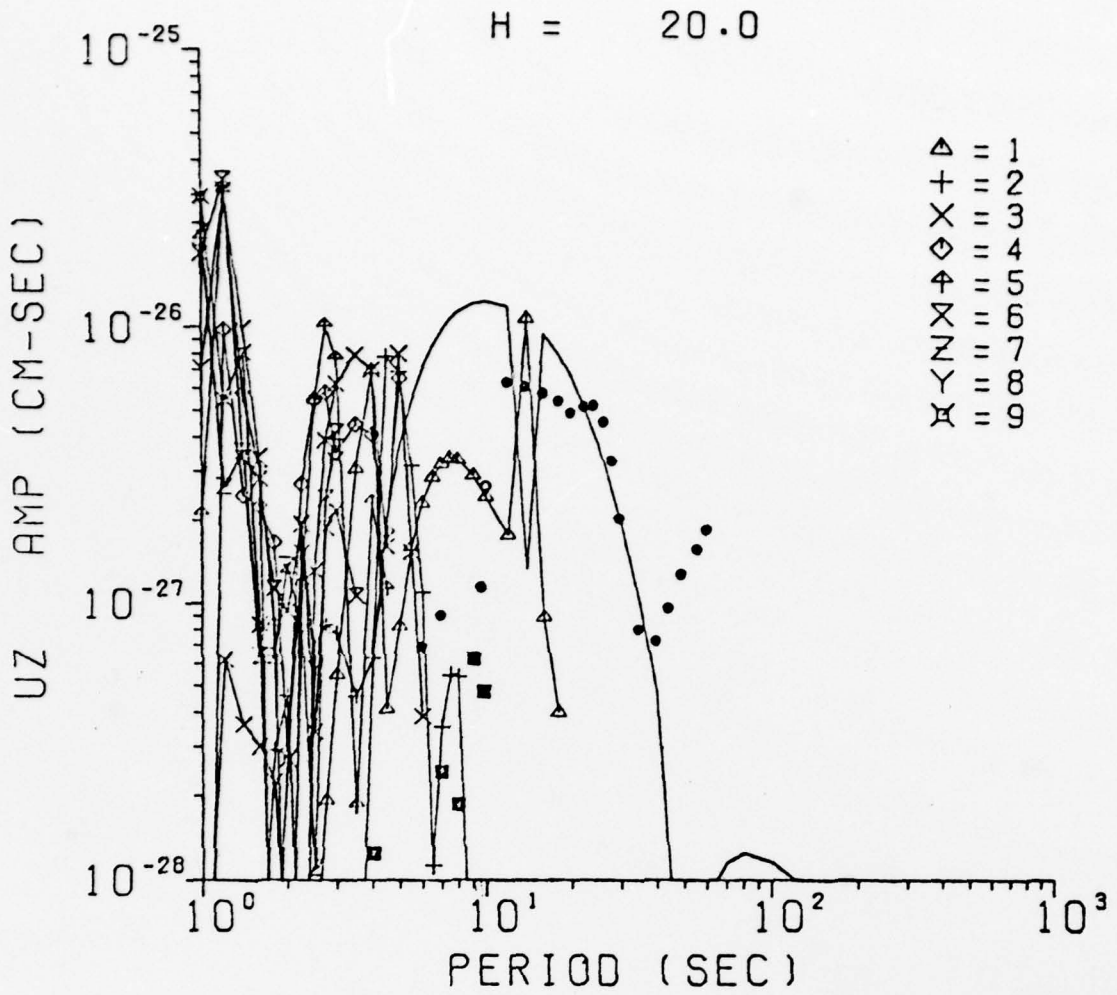

Figure 4. Observed and theoretical spectra for the same case as Figure 3 except that the source depth is assumed to be 20 km.

higher-mode attenuation data. Frequency-dependent models will be sought which will also explain the attenuation of regional phases such as Lg.

References

Bucher, R.L., and R.B. Smith, Crustal structure of the eastern Basin and Range province and the northern Colorado Plateau from phase velocities of Rayleigh waves, in Geophys. Mono. 14, The Structure and Physical Properties of the Earth's Crust, 57-70, AGU, Washington, D.C., 1971.

Levshin, A.L., and Z.A. Yanson, Surface waves in vertically and radially inhomogeneous media, Algorithms for the interpretation of seismic data, Vo. 5, 147-177, Moskow, 1971.

McKenzie, D., Active tectonics in the Mediterranean region, Geophys. J. Roy. Ast. Soc., 30, 109-185, 1972.

SECURITY CLASSIFICATION OF THIS PAGE (When Data Entered)

REPORT DOCUMENTATION PAGE		READ INSTRUCTIONS BEFORE COMPLETING FORM
1. REPORT NUMBER AFOSR-TR- 79-0692	2. GOVT ACCESSION NO.	3. RECIPIENT'S CATALOG NUMBER
4. TITLE (and Subtitle) Research in Seismology		5. TYPE OF REPORT & PERIOD COVERED Interim
		6. PERFORMING ORG. REPORT NUMBER
7. AUTHOR(s) Brian J. Mitchell Otto W. Nuttli		8. CONTRACT OR GRANT NUMBER(s) F49620-79-C-0025
9. PERFORMING ORGANIZATION NAME AND ADDRESS Dept. of Earth & Atmospheric Sciences Saint Louis University St. Louis, Missouri 63156		10. PROGRAM ELEMENT, PROJECT, TASK AREA & WORK UNIT NUMBERS ARPA Order: 3291-2 Program Element: 61101E Code No.: 9D60
11. CONTROLLING OFFICE NAME AND ADDRESS Advanced Research Projects Agency 1400 Wilson Blvd. Arlington, Virginia 22209		12. REPORT DATE April 23, 1979 13. NUMBER OF PAGES 82
14. MONITORING AGENCY NAME & ADDRESS(if different from Controlling Office) Air Force Office of Scientific Research Bolling Air Force Base Washington, D.C. 20332		15. SECURITY CLASS. (of this report) Unclassified 15a. DECLASSIFICATION/DOWNGRADING SCHEDULE

16. DISTRIBUTION STATEMENT (of this Report)

Approved for public release. Distribution unlimited.

17. DISTRIBUTION STATEMENT (of the abstract entered in Block 20, if different from Report)

18. SUPPLEMENTARY NOTES

19. KEY WORDS (Continue on reverse side if necessary and identify by block number)

Attenuation	Spectra	Surface waves
Asia	Higher modes	Lg
Q		

20. ABSTRACT (Continue on reverse side if necessary and identify by block number)

The attenuation of crustal phases in southern Asia is on the average intermediate between that of Iran and eastern North America. To distances of 1000 km the phases Pg and Lg have the largest amplitudes, but at larger distances P and Sn dominate. Higher mode surface wave studies at periods between 1 and 10 seconds indicate the shear wave Q in the crust depends upon frequency, at least at periods of less than 5 seconds.

DD FORM 1473